HHS Public Access

Author manuscript

Neuroimage. Author manuscript; available in PMC 2021 February 09.

Published in final edited form as:

Neuroimage. 2020 December ; 223: 117346. doi:10.1016/j.neuroimage.2020.117346.

Cross-species functional alignment reveals evolutionary hierarchy within the connectome

Ting Xu[a,1,*], **Karl-Heinz Nenning**[b,1], **Ernst Schwartz**[b], **Seok-Jun Hong**[a], **Joshua T. Vogelstein**[c], **Alexandros Goulas**[d], **Damien A. Fair**[e], **Charles E. Schroeder**[f,g], **Daniel S. Margulies**[h], **Jonny Smallwood**[i,j], **Michael P. Milham**[a,f,1], **Georg Langs**[b,k,1]

[a]Center for the Developing Brain, Child Mind Institute, New York, NY, USA

[b]Computational Imaging Research Lab, Department of Biomedical Imaging and Image-guided Therapy, Medical University of Vienna, Austria

[c]Department of Biomedical Engineering, Institute for Computational Medicine, Kavli Neuroscience Discovery Institute, Johns Hopkins University, MD, USA

[d]Institute of Computational Neuroscience, University Medical Center Hamburg-Eppendorf, Hamburg University, Hamburg, Germany

[e]Advanced Imaging Research Center, Oregon Health & Science University, Portland, OR, USA

[f]Center for Biomedical Imaging and Neuromodulation, Nathan Kline Institute, Orangeburg, NY, USA

[g]Departments of neurosurgery and Psychiatry, Columbia University College of Physicians and Surgeons, New York, NY, USA

[h]Centre National de la Recherche Scientifique (CNRS) UMR 7225, Frontlab, Institut du Cerveau et de la Moelle Epinière, Paris, France

[i]Department of Psychology, Queen's University, Kingston, Ontario, Canada

[j]Psychology Department, University of York, York, UK

[k]Computer Science and Artificial Intelligence Laboratory, Massachusetts Institute of Technology, Cambridge, MA, USA

Abstract

[*]Corresponding author. ting.xu@childmind.org (T. Xu).
[1]These authors contributed equally to this work.

CRediT authorship contribution statement

Ting Xu: Conceptualization, Methodology, Formal analysis, Visualization, Writing - original draft, Writing - review & editing. **Karl-Heinz Nenning:** Conceptualization, Methodology, Formal analysis, Visualization, Writing - original draft, Writing - review & editing. **Ernst Schwartz:** Methodology, Writing - review & editing. **Seok-Jun Hong:** Writing - review & editing. **Joshua T. Vogelstein:** Methodology. **Alexandros Goulas:** Writing - review & editing. **Damien A. Fair:** Writing - review & editing. **Charles E. Schroeder:** Writing - review & editing. **Daniel S. Margulies:** Conceptualization, Methodology, Writing - review & editing. **Jonny Smallwood:** Conceptualization, Writing - review & editing. **Michael P. Milham:** Conceptualization, Writing - review & editing. **Georg Langs:** Conceptualization, Methodology, Writing - review & editing.

Supplementary materials

Supplementary material associated with this article can be found, in the online version, at doi: 10.1016/j.neuroimage.2020.117346.

Evolution provides an important window into how cortical organization shapes function and vice versa. The complex mosaic of changes in brain morphology and functional organization that have shaped the mammalian cortex during evolution, complicates attempts to chart cortical differences across species. It limits our ability to fully appreciate how evolution has shaped our brain, especially in systems associated with unique human cognitive capabilities that lack anatomical homologues in other species. Here, we develop a function-based method for cross-species alignment that enables the quantification of homologous regions between humans and rhesus macaques, even when their location is decoupled from anatomical landmarks. Critically, we find cross-species similarity in functional organization reflects a gradient of evolutionary change that decreases from unimodal systems and culminates with the most pronounced changes in posterior regions of the default mode network (angular gyrus, posterior cingulate and middle temporal cortices). Our findings suggest that the establishment of the default mode network, as the apex of a cognitive hierarchy, has changed in a complex manner during human evolution – even within subnetworks.

Keywords

Cross-species alignment; Joint embedding; Evolution; Hierarchy; Default mode network

1. Introduction

The human brain differs from other species in both scale and organization (Barton and Harvey, 2000; Krubitzer, 2009; Sousa et al., 2017; Van Essen et al., 2018). One way to understand the emergence of its unique functions is through comparative neuroimaging across different species (Mantini et al., 2012; Mars et al., 2014; Reid et al., 2016; Rilling, 2014; Van Essen et al., 2018). Evidence of similarities between neural systems in different species are assumed to reflect functions that may be relatively conserved across evolution (Kaas, 2012a; Krubitzer, 2007). In contrast, regions showing the greatest changes between humans and other species highlight neural changes that may account for features of cognition unique to humans (Ardesch et al., 2019; Buckner and Krienen, 2013; Patel et al., 2015). Traditionally, cross-species comparisons have depended on the identification of anatomical anchors (e.g. key cortical landmarks or common white matter tracts) and corresponding cortical features (e.g. myelination) in humans versus other species (Eichert et al., 2019; Goulas et al., 2014; Mars et al., 2018b; Van Essen et al., 2018; Van Essen and Dierker, 2007). These approaches have successfully identified putative homologous regions that are common to primates including macaques, marmosets and chimpanzees and humans (Chaplin et al., 2013; Donahue et al., 2018; Eichert et al., 2019; Van Essen and Dierker, 2007). These anatomy-based approaches have revolutionized our understanding of the organization of the mammalian cortex and suggest that the basic processes linked to moving and perceiving are relatively conserved across species (Hopkins et al., 2014; Krubitzer, 2007).

Although common anatomical landmarks highlight similarities in how the brain supports interactions with the immediate environment across primate species, evolution has also emphasized cognitive capabilities less closely tied to the processing of information in the

'here and now' (Donahue et al., 2018; Hill et al., 2010; Murphy et al., 2018; Smallwood et al., 2013; Sormaz et al., 2018). These include the ability to understand the hidden mental states of conspecifics (i.e. theory of mind), to solve problems in a creative manner, to use language to communicate intentions, and to explicitly imagine times and places not immediately available to perception (Berwick et al., 2013; Byrne, 1995; Hage and Nieder, 2016; Mansouri et al., 2017; Poerio et al., 2017). In humans, many of these processes are related to neural processing in transmodal regions of the so-called default mode and frontoparietal networks (Andrews-Hanna et al., 2014; Margulies et al., 2016). Understanding cross-species differences in transmodal regions is challenging because (i) these regions often lack clear anatomically-defined cross-species homologues (Buckner and Krienen, 2013; Mantini et al., 2013; Van Essen and Dierker, 2007) and (ii) evolution has not led to uniform cortical expansion, but has reorganized function in a heterogeneous manner that changes how regions communicate with one another (e.g. mosaic processes) (Barton and Harvey, 2000; Gómez-Robles et al., 2014; Smaers and Soligo, 2013).

A comprehensive account of how evolution has shaped cortical organization in humans, therefore, requires the mapping of how function has changed in regions of cortex where there are relatively few well-defined physical landmarks and where we may anticipate the largest cross-species differences. Contemporary accounts suggest that mammalian neural processing is organized along multiple hierarchies describing how information from distinct neural populations are integrated and segregated across the cortex (Buckner and Krienen, 2013). One important hierarchy reflects the process through which information from unimodal systems are bound together to form abstract, cross-modal, representational codes assumed to be important for multiple aspects of higher-order cognition (Mesulam, 1998). Recent observations suggest that this hierarchy is partly reflected in the intrinsic geometry of the cortex, such that regions of transmodal cortex occupy locations equidistant from unimodal systems (e.g. visual, auditory, and sensorimotor cortices) (Margulies et al., 2016). This hierarchy enables the transmodal cortex to integrate multiple sources of input and thus may underlie important aspects of higher-order cognitive functions.

To understand how evolution has shaped neural function in regions of the transmodal cortex, our study leverages recent advances in representing functional organization in a high-dimensional common space (Margulies et al., 2016). We build on prior work that shows it is possible to align across species by comparing neural activity during movie watching (Mantini et al., 2012) and that at a coarse level of analysis, similar neural hierarchies are observed in different primate species (Chaplin et al., 2013; Van Essen et al., 2018; Van Essen and Dierker, 2007). Since we were interested in charting functional differences in transmodal regions in different species we used resting-state functional connectivity data collected in two primate species (human and macaques) (Milham et al., 2018). Our connectome comparative method, which we refer to as *joint-embedding*, extracts the most similar dimensions of functional organization from both humans and macaques. Using this approach, we are able to empirically determine whether regions that in humans fall towards the apex of the unimodal-transmodal hierarchy have a different functional profile in macaques and thus shed important light how evolution has shaped neural function in regions that may be important for important aspects of human cognition.

2. Methods

2.1. Macaque data

All datasets in this study were from openly available sources. The macaque data stemmed from the recently established PRIME-DE (http://fcon_1000.projects.nitrc.org/indi/indiPRIME.html) (Milham et al., 2018). Three cohorts of macaque samples from PRIME-DE have been included in the present study. 1) *Oxford data (anesthetized).* The full dataset consisted of 20 rhesus macaque monkeys (macaca mulatta) scanned on a 3T with a 4-channel coil (Noonan et al., 2014). The resting-state fMRI (R-fMRI) data were collected while the animals were under anesthesia with 2 mm isotropic resolution, TR=2 s, 53.3 min (1600 volumes). No contrast-agent was used during the scans. Nineteen macaques with successful preprocessing and surface reconstruction were included in the present study (all males, age=4.01±0.98, weight=6.61 +/−2.04). 2) *UC-Davis data (anesthetized).* The full dataset consisted of 19 rhesus macaque monkeys (macaca mulatta) scanned on a Siemens Skyra 3T with a 4-channel clamshell coil. The resting-state fMRI data were collected with 1.4 × 1.4 × 1.4 mm resolution, TR=1.6s, 6.67 min (250 volumes) under anesthesia. No contrast-agent was used during the scans. Nineteen macaques were included in the present study (all female, age=20.38±0.93, weight=9.70±1.58). 3) *Newcastle data (awake).* The full data set consisted of 14 rhesus macaque monkeys (macaca mulatta) scanned on a Vertical Bruker 4.7T primate dedicated scanner (Baumann et al., 2015, 2011; Poirier et al., 2017; Rinne et al., 2017; Schönwiesner et al., 2015; Slater et al., 2016; Wilson et al., 2015). We included 10 animals (8 males, age=8.28±2.33, weight=11.76±3.38) who were scanned awake. The fMRI session was acquired with 1.2 × 1.2 × 1.2 mm resolution, TR=2s, 8.33-min per scan (250 volumes x 2 scan) for each animal. No contrast-agent was used during the scans.

2.2. Human data

The human dataset was selected from the unrelated participants of the HCP (Glasser et al., 2013). We selected the R-fMRI data from the unrelated participants (n = 178) in the HCP S500 release (Glasser et al., 2013). The first R-fMRI scan acquired on day one has been included in the current analysis, containing a 15-min run (phase encoding left-right) for each participant. The details of the acquisition and the preprocessing can be found at https://www.humanconnectome.org.

To ensure replicability, randomly split the human data into two subsets (subset HCP1, n=93, 46 females, age=29.23±3.49; subset HCP2, n=94, 36 females, age=28.99±3.43). These two subsets were grouped into two human and anesthetized macaque comparisons (HCP1-Oxford, HCP2-UCD) and two human and awake macaque comparisons (HCP1-Newcastle, HCP2-Newcastle). The following interspecies alignment analyses were replicated in all four comparison samples. We focus on the HCP1-Oxford sample in the main results and present the three other comparisons in Supplementary materials.

2.3. Preprocessing

The macaque monkey data were preprocessed using the customized HCP-like pipeline from DAF's laboratory and the Computational Connectome System (Xu et al., 2015). The details

of the data preprocessing were described previously (Xu et al., 2019, 2018). Briefly, the R-fMRI data were preprocessed including temporal compression, motion correction, 4D global scaling, nuisance regression using white matter (WM), and cerebrospinal fluid (CSF) signal and Friston-24 parameter models, bandpass filtering (0.01–0.1 Hz), detrending and co-registration to the native anatomical space. The data were then projected to the native mid-cortical surface and smoothed along the surface with FHWM=3mm. Finally, the preprocessed data were down-sampled to a 10k (10,242 vertices) resolution surface. Similar with the macaque preprocessing, the human data have been minimally preprocessed in the HCP pipeline in addition with the bandpass filtering (0.01–0.1 Hz), spatial smoothing along the surface (FWHM=6mm) and downsampling to the 10k (10,242 vertices) mid-cortical surface (Autio et al., 2019; Donahue et al., 2016).

2.4. Cross-species landmarks

The landmarks were selected based on the milestone study from Van Essen' group (Van Essen and Dierker, 2007) and recent cross-species comparison based fMRI studies (Mars et al., 2011; Neubert et al., 2014; Sallet et al., 2013). Only potential landmarks that have been reported in at least two studies were included in the current work. The final set included 27 landmarks (Table S1). The area definition in humans was based upon the most recent multi-modal human parcellation (Glasser et al., 2016). For the landmark area in macaque, we first collected the area definitions from seven macaque atlases and used the vertices that at least overlapped within two atlases for the final macaque landmarks (Felleman and Van Essen, 1991; Ferry et al., 2000; Lewis and Van Essen, 2000; Markov et al., 2014; Paxinos and Franklin, 2012; Preuss and Goldman-Rakic, 1991; Van Essen et al., 2012). The details of the studies used to define the landmarks and the atlas references were listed in Table S1.

2.5. Joint-embedding

In previous work on manifold alignment, spectral embedding (e.g. diffusion maps) has demonstrated the ability to align the connectivity structure across individuals (Coifman and Lafon, 2006; Nenning et al., 2017). Recently, this approach has been used to characterize the connectivity topographies and capture the cortical gradients spanning along the unimodal (visual and somatomotor cortices) and transmodal regions (association cortex) within each species in human and macaque monkey (Haak et al., 2018; Margulies et al., 2016). Here, in order to align human and macaque monkey cortex, the challenge is to extract comparable cross-species components, rather than applying embeddings for each species individual and subsequently performing component matching. To address this challenge, we propose a joint-embedding approach to compute matched components (referred to as 'gradients') in human and macaque monkey.

First, we constructed a joint similarity matrix by concatenating within- and cross-species similarities of connectivity patterns (Fig. 1A), as defined in

$$\boldsymbol{W}_{human} = \left[\boldsymbol{W}_{human}, \boldsymbol{W}_{human\_to\_monkey}; \boldsymbol{W}_{monkey\_to\_human}, \boldsymbol{W}_{monkey}\right]$$

The diagonal within-species similarity matrices (W_{human} and W_{monkey}) are calculated using cosine similarity of row-wise thresholded functional connectivity at each vertex in each

species (Margulies et al., 2016). The functional connectivity was calculated at the group-level by averaging the individual connectivity matrix first within each of the comparison samples. The off-diagonal cross-species similarity matrix $W_{human\_to\_monkey}$ (and its transpose $W_{monkey\_to\_human}$) was calculated based on the landmark similarity profile of the functional connectivity pattern (Fig. S1). Specifically, similar to a previous study from Mars (Mars et al., 2018b), we first computed the thresholded vertex-to-vertex connectivity matrix (C_{human} and C_{monkey}) and averaged the vertex-wise connectivity to each landmark respectively to generate the vertex-to-landmark connectivity matrix (L_{human} and L_{monkey}) for each species. Based on these two connectivity matrices profile, we calculated the vertex-to-landmarks similarity matrix (S_{human} and S_{monkey}) within each species. That is, for each vertex within a species, the row i of matrix S is defined as the cosine similarity between row i of C and row i of L. Note that the 27 landmarks were matched homologous areas between human and macaque monkey, in other words, the columns of S_{human} and S_{monkey} are matched. Then we measured the cross-species similarity matrix $W_{human\_to\_monkey}$ (and its transpose $W_{monkey\_to\_human}$) by comparing the similarity pattern to the homologous landmarks across species. To determine the threshold for the connectivity matrix within each species, we tested the sparsity thresholds at 1% to 10% and examined the distance of matched homologous landmarks between human and macaque in the resultant gradient space. The sparsity threshold 1% generated the most similar cross-species gradients and was employed in the final analysis.

Next, we applied the diffusion embedding algorithm on the concatenated matrix W, resulting in a set of components (Coifman and Lafon, 2006). Of note, the joint similarity matrix W is a symmetric matrix across species. The diagonal block matrices contain the within species connectivity profiles in human and macaque, encoding backbone connectivity structure (thresholded at top 1%), while the off-diagonal matrices provide a coupling across species via the comparable landmarks. Therefore, for each of the obtained components, the first half of entries correspond to the human vertices and the second half macaque vertices (Fig. 1A). Each component provides a set of matched cortical gradients covering the human and macaque cortices, which can be served as one of the dimensions of the common cross-species coordinate space. We first extracted the top 200 components and selected only the top k components to construct a gradient pool for the following surface matching procedure. Here, k is determined as the inflection point of eigenvalues (lambdas) on the scree plot (Fig. S2A). Twenty-five components (i.e. gradients) were selected in the HCP1-Oxford comparison sample (21 for HCP1-Newcastle, 18 for HCP2-UCDavis, 21 for HCP2-Newcastle).

Finally, we used the gradients from the above gradient pool as the surface features and aligned the human and macaque cortical surface with Multimodal Surface Matching (MSM) (Robinson et al., 2014). In order to avoid misalignment in the medial wall between human and macaque, we added the medial wall mask as an additional feature into MSM. The MSM configuration parameters ‘config_MSMsulc_pairwise’ was used in alignment. To optimize the number of gradients for the final alignment, we entered the top 5, 10, 15, and 20 gradients in MSM and determined the performance using 27 landmarks labels as the inspection standard. Top 15 components were finally selected for the alignment in comparison samples. Accordingly, these 15 components were used as gradient profiles to

build the common coordinate space between human and macaque monkey (Fig. S3). It is worth noting that one of the macaque replication samples was scanned awake (Newcastle). To evaluate the state effect in the cross-species comparison, we calculated the similarity of the gradients' profiles from HCP1-Newcastle cross-species analyses to those generated from the HCP1-Oxford cross-species analyses (Fig. S4). The Procrustes linear transform was applied to the raw gradients to match the order between two the two different analyses (awake human and macaque: HCP1-Newcastle, awake human and anesthetized macaque: HCP1-Oxford). The high similarity was observed in human gradients after the Procrustes transform (mean r=0.89). For macaque, the gradients were less similar between the anesthetized (Oxford) and awake (Newcastle) samples, though still relatively high (mean r=0.68).

We examined the alignment performance by applying the surface deformation to the myelin sensitive maps (i.e. T1w/T2w) and compared the aligned myelin prediction map with the actual T1w/T2w estimation in aligned species (Fig. 2D). In addition, several well-established human and macaque parcellations and networks can be registered well from human to macaque, vice versa (Fig. S5A). We also calculated the cross-species similarity matrix based on 15 gradient profiles at each vertex. We demonstrated the parcel-wise similarity matrix using the most recent multimodal parcellations for the human and its aligned human-to-macaque parcellation for the macaque (Fig. S6A). It can be seen that in general the cross-species similarity revealed greater similarity within networks than between networks (Fig. S6A).

2.6. Functional Connectivity Homology Index (FCHI)

In order to quantify cross-species regional similarities of functional organization in the functional common space, we further developed the *Functional Connectivity Homology Index* (FCHI, Fig. 2A). Specifically, for each pair of coordinates identified as corresponding between species in MSM, we quantified the maximum cosine similarity of 15 gradients as FCHI across species within corresponding searchlights (radius = 12 mm on the midthickness surface). The searchlight approach mitigates the possibility of excessive topological constraints from MSM, while limiting the identification of matches that are unfeasible (e.g. MT and fusiform face area [FFA] in Fig. S5B). The maximum similarity within the corresponding searchlight quantified the highest likelihood that the functional gradients at each vertex in humans can be represented in macaque (Fig. 2B) and vice versa (Fig. S6B).

2.7. The activation possibility strength of BrainMap cognitive component

To quantify the relationship between functional homology and cognitive function, we employed a similar analysis as described in recent studies (Margulies et al., 2016; Wang et al., 2019). The human cognitive functions were represented using the activation possibility maps of 12 cognitive components from a previous large-scale meta-analysis based on the BrainMap database (Yeo et al., 2015). Specifically, we first grouped the macaque-to-human FCHI map into 10-percentile bins. For each of 12 cognitive components, the activation strength was normalized by dividing the sum of each component' activation possibility and then sum within each of the 10 bins. The score in the heatmap represents the total activation possibility associated with a given cognitive component within each of the 10-percentile bin

regions. The cognitive components were ordered based on the activation strength weighted by the log scale of percentile.

2.8. Evolutionary deformation and area expansion

The evolutionary surface expansion was calculated at each vertex based on the correspondence established in MSM. Specifically, we first estimated the vertex-wise surface area of the 32k standard surface mesh in native space for each of human and macaque individuals. We then resampled and smoothed (FWHM=6 mm in human and FWHM=3 mm in macaque) the area estimations to 10k surface using areal interpolation (Winkler et al., 2012). Next, the individual area maps were averaged across all the individuals to generate area maps for each of human (n=187) and macaque samples (n=48). After that, we estimated the macaque surface area at each of corresponding human vertices using the registration sphere in MSM (Winkler et al., 2012). The final relative area expansion was calculated by dividing the human surface area by the macaque surface area at each vertex on the human surface. Similarly, we calculated the relative area at each vertex on the macaque surface, suggesting the starting points of the expansion origin from macaque to human. To further demonstrate the evolutionary direction on the surface, we calculated macaque-to-human deformation vectors. To facilitate the visualization in highly folded regions (e.g. insular), we used the 'very_inflated' surface for both human and macaque monkey. Specifically, we identified the macaque-to-human coordinates for each of the vertices corresponding to the very_inflated macaque surface using MSM registration sphere. Next, we calculated the vector based on the MSM aligned coordinates from macaque to human. The length of the vector represents the strength of the evolutionary deformation along the direction from macaque to human surface.

3. Results

3.1. Joint-embedding approach captures the common brain architecture across species

To construct a common functional space for cross-species comparison, we extended the spectral embedding-based approach for mapping connectivity topographies (Haak et al., 2018; Langs et al., 2010; Margulies et al., 2016; Nenning et al., 2017). The framework of this cross-species method is visualized and introduced in the form of videos (http://fcon_1000.projects.nitrc.org/indi/PRIME/je_alignment.html).

In brief, we applied spectral embedding to a joint similarity matrix rather than computing embeddings for each species individually and subsequently performing alignment (Fig. 1). The joint similarity matrix was constructed by concatenating the following four submatrices: 1) two within-species similarity matrices (one for each species located along the diagonal), calculated using cosine similarity of thresholded functional connectivity at each vertex in each species, and 2) two off-species similarity matrices (macaque-to-human and its transpose human-to-macaque), calculated by cosine similarity of functional connectivity at each vertex with each of matched homologous landmarks, and treated as off diagonal matrices (Fig. 1A and B, Table S1) (Mars et al., 2011; Neubert et al., 2014; Sallet et al., 2013; Van Essen and Dierker, 2007). The joint-embedding results in a representation of functional connectivity shared between the two species in the form of components.

Specifically, we extracted the matched components for both species, where each dimension represents the common feature along the respective embedding axis. We refer to this common space as the joint-embedding space and each dimension (component) as a 'gradient'. The top 15 components were found to meet our minimum landmark alignment criteria (see Methods for details) and thus were retained for further analysis. We validated the matched inter-species common space by examining the similarity of the presumably anatomical landmarks in this space (Fig. 1C, Fig. S2). The Pearson correlations of the landmarks in joint-embedding space are all in the top 5% percentile of the pairwise correlations between human and macaque (ranging from r=0.877 [FEF] to r=0.999 [V1], p<0.001; Fig. S3).

3.2. The joint embedding highlights homologous regions and aligns myelin distribution across species

Our first set of analyses are aimed at establishing cross-species alignment using joint-embedding gradients. To demonstrate that the gradients can serve as common space for both species, we show that they capture the similarity in location of the well documented cross-species landmarks (Fig. 1C). After generating the joint-embedding space we projected the results (i.e. gradients) back onto human and macaque cortical surfaces. As shown in Fig. 1D, the homologous regions for both species are the apex of the same gradient (e.g. V1 as a negative nadir in gradient 1, motion-selective visual area (MT) as the positive apex in gradient 3) or occupy similar areas within the spectrum of a gradient (e.g. MT in gradient 1, V1 in gradient 3).

Next, we examined whether the joint embedding gradients provide a compact description of the distribution of myelin in both species. To establish the surface deformation between macaque and human cortex, the selected top 15 gradients as functional mesh features in Multimodal Surface Matching (MSM, Fig. 1E) for the surface registration between human and macaque (details of the model are in Methods) (Nenning et al., 2017; Robinson et al., 2014). We validated the alignment generated by joint embedding by testing its ability to generate a T1w/T2w (i.e. myelin sensitive) map for each species though predicting the T1w/T2w based on the other species following the established alignment (Glasser and Van Essen, 2011). We applied the surface human-to-macaque alignment to the myelin map that was calculated from HCP data and compared the aligned T1w/T2w predicated map to the actual macaque T1w/T2w map calculated based on Yerkes-19 template sample (Fig. 1F) (Donahue et al., 2016). The predicted map was similar to the actual T1w/T2w map (r=0.622, p<0.001 corrected). We also applied the macaque-to-human alignment to predict the human T1w/T2w using the macaque T1w/T2w map, yielding a similar, although weaker association (r=0.574, p<0.001 corrected).

3.3. Cross-species Functional Connectivity Homology Index (FCHI)

Having established that our cross species embedding adequately captures both the known homologous landmarks, and species-specific distributions of myelin in a reasonable manner, we next considered whether our approach can provide a description of how neural function differs between macaques and humans. To quantify regional similarities in functional organization across species, we developed the Functional Connectivity Homology Index

(FCHI, Fig. 2A). For each pair of coordinates identified as corresponding between species using MSM, the FCHI quantifies the maximum similarity of functional gradient profiles across species within corresponding searchlights (radius = 12 mm along the surface). An advantage of using a searchlight approach is that it mitigates the possibility of excessive topological constraints from MSM, while limiting the identification of matches that are unfeasible. Fig. S5B demonstrates how the searchlight approach in identifying areas across species when their locations are anatomically decoupled (e.g. MT and fusiform face area) (Tsao et al., 2008; Yovel and Freiwald, 2013). The maximal similarity within the corresponding searchlight evaluated the highest likelihood that the functional gradients at each vertex in humans can be represented in macaque (Fig. 2B) and vice versa (Fig. S6B). These patterns were replicated in another three comparison samples and obtained the highly similar FCHI map using the awake macaque samples as well (Fig. S7).

3.4. Connectome wide differences in the organization of neural functions as demonstrated by the FCHI

The FCHI reveals the upper bounds of interspecies alignment that can be achieved based on functional organization when going from human-to-macaque, and from macaque-to-human. Here, the functional connectivity homology indices reflect the degree of common functional organization across both species. As shown in Fig. 2B, the cross-species homology index was highest in sensory areas including early visual cortices, the MT, auditory area, the fusiform face area (FFC) and the dorsal somatomotor areas. As expected, the prefrontal cortex, which is greatly expanded in human relative to the macaque, exhibited a relatively low FCHI. Importantly, a large set of high-order transmodal regions showed the lowest degree of homology index, in particular in dorsolateral prefrontal cortex (dlPFC), lateral temporal cortex (LTC), parietal gyrus regions (PG), and posterior medial cortex (PMC). This set of regions corresponds well with what is known as the default mode network (DMN) in humans. Of particular interest, the FCHI is at zero in PG regions, indicating that no regions can be found in macaques that have a functional organization similar to that of PG regions in humans. To quantify the FCHI at the level of networks, we averaged macaque-to-human similarity strength in each of seven human networks (Fig. 2C) (Yeo et al., 2011). The sensory networks, in particular the visual network, showed the highest FCHI, followed by the attention, limbic, frontoparietal networks with a moderate degree of homology index; the DMN showed the lowest homology index. Next, we examined whether cross species similarity in neural functions that are described by the FCHI are related to the cortical distribution of myelin estimated by T1w/T2w. We found that the T1w/T2w was significantly associated with the FCHI such that greater similarity between species was observed in regions that tended to be high in estimated levels of myelination (Fig. 2D, r=0.428, p<0.001, corrected). Together these analyses suggest that in functional terms regions that fall towards the apex of a unimodal-transmodal hierarchy in humans tend to have the greatest functional differences in macaques and that this difference may link to lower levels of myelin.

To evaluate the extent to which differences in FCHI along the cortical hierarchy were driven by the cortical geometry and distances to the landmarks, we measured the geodesic distance at each vertex to the nearest landmark and found a relatively low correlation (r=−0.331, Fig. S8A). It is worth noting that only the regions with the longest distance (dark red line in Fig.

S8A, right panel) exhibited the skewed low FCHI scores. This suggested that the potential impact of the cortical geometry was not global but mainly driven by regions far away from the landmarks (i.e. PMC and lateral temporal lobe). We further performed a leave-one-out analysis and found that the FCHI map was highly stable across landmarks. All leave-one-out FCHI maps showed high similarity with the original FCHI map, with only validation yielding a value below 0.9 (A1: r=0.769, Fig. S8B).

In addition, we also evaluated how each of the gradients contribute to the cortical hierarchy of FCHI pattern. To this end, we calculated the FCHI based on the subset of the gradients (i.e. #1–5, #2–6, …, and #11–15) and compared to the FCHI map based on the full set of gradients (Fig. S9). We found that the first 5 gradients generated the highest similarity of FCHI pattern (r=0.864), followed by the second 5 gradients (r=0.822) and the third 5 gradients (r=0.625). The first 5 gradients also showed higher FCHI scores as compared to the last 5 gradients. These findings suggested that the early gradients captured more common functional modes between species and dominated spatial profile of the FCHI map.

3.5. The cross-species Functional Connectivity Homology Index characterizes the distributed local sensory hierarchies

Our analysis so far suggests that at a broad connectome wide level the functional differences between humans and macaques emerge in a hierarchical manner from unimodal to transmodal cortex. Next we examined whether the FCHI also can describe more local (i.e., within system) variations in cross-species functional organization. Here we focus on examples from the visual and somatomotor systems, as their hierarchical organizations are among the best understood (Buckner and Krienen, 2013; Felleman and Van Essen, 1991).

The distribution of the FCHI in the visual system can be seen in Fig. 3. It can be seen that in the early visual system, the primary visual area, V1, has the highest homology index, followed by the secondary visual area V2, the third visual area V3, and V3A; the lowest functional homologue values were observed in V4. This pattern suggests that FCHI reflects previously established visual processing order with increasing eccentricity (Felleman and Van Essen, 1991). Beyond early visual areas, in the ventral pathway, we found that the mean Functional Connectivity Homology Index progressively decreased with the complexity of information across ventral stream labeled by Brodmann Atlas areas: 17, 18, 19, 37, 20, 21 (Ungerleider and Haxby, 1994). Notably, consistent with the tethering hypothesis, which suggests that V1 and MT were both “molecular anchors ” for evolutionary processing, the FCHI for MT was comparable to V1, with lower scores being noted in surrounding areas (Fig. 3C). In somatomotor areas, the FCHI varied along the dorsal-ventral axis of somatotopic mapping (Glasser et al., 2016). The lower limb (i.e. foot) area has the greatest homology index, followed by trunk (i.e., body), and upper limb (i.e., hand); Such dorsal-to-ventral hierarchy from the lower limb to the upper limb may reflect brain adaptations for human bipedalism where the hands are more highly distinguished – for example with relatively long thumb for high precision grip in humans (Almécija et al., 2015; Oya et al., 2020). The ventral areas, eye and face/tongue areas showed the lowest FCHI (Fig. 3E). This might reflect the different evolutionary trajectory between human and NHP, as these areas

evolved unique speech motor control for language in human evolution (Toda and Kudo, 2015).

Having identified that the FCHI varies along local hierarchies, we evaluated whether this effect could be accounted for by cortical geometry rather than functional connectivity from fMRI data. To assess this, we repeated our analyses using the cortical distance matrices rather than functional connectivity data and calculated the homology index of intrinsic cortical geometry between human and macaque (Fig. S10). Notably, only in early visual areas did the geometry-based homology index demonstrate an association with hierarchy level, decreasing from V1 to higher-order areas. These results confirm that aside from early visual cortex, our primary findings above are driven by functional organization rather than cortical geometry.

3.6. The FCHI reveals the modular specialization of the subsystems in attention and frontoparietal networks

Our examination of transmodal cortex began with the frontoparietal and attention networks. In humans the frontoparietal and attention networks have been suggested to be dissociable into pairs of networks that are dissociable with respect to their functional proximity to unimodal versus transmodal systems (i.e. the default mode network) (Braga and Buckner, 2017; Dixon et al., 2018). In our analysis, the FCHI readily distinguished between the frontoparietal network-A (FN-A) and frontoparietal network-B (FN-B). Specifically, we found that FN-A which has stronger connections to the default mode network and exhibited lower FCHI scores (Fig. 4A); while, FN-B, which is more connected to the dorsal attention network in humans (Braga and Buckner, 2017; Dixon et al., 2018), exhibited higher scores. Similarly, a lower FCHI was observed in dorsal attention network-A (dATN-A) than dATN-B, which is more directly connected to retinotopic visual regions (Braga and Buckner, 2017). Finally, a similar pattern was observed in the two subnetworks in ventral attention network. Within both the frontoparietal and attention systems, therefore, we found a consistent pattern that the FCHI was lower in networks that are functionally less closely linked to unimodal systems (Caspari et al., 2015).

3.7. The evolutionary hierarchy of subregions in default mode networks

Next, we examined the cross-species similarity of the DMN, which in humans is located at the apex of the principle cognitive hierarchy (Margulies et al., 2016). Similar to the frontoparietal network, the DMN exhibited overall differences in the FCHI among its subsystems (Andrews-Hanna et al., 2014, 2010; Braga and Buckner, 2017). In particular, the medial temporal system had the highest FCHI, the core DMN the lowest, and dorsal medial system intermediate (Fig. 4B). Across the systems, the angular gyrus (PG), posterior medial cortex (PMC) and the lateral temporal cortex (LTC) had the lowest FCHI scores (Fig. 4B).

In humans it has been recently established that regions within the DMN, primarily within the core DMN subregions, contain information regarding patterns of functional connectivity across the cortex as a whole (Kernbach et al., 2018). To understand whether cross species similarity in functional organization reflects this fine-grained distinction, we tested for associations between the FCHI and regions that reflect a high level of ‘importance’ within

the DMN as identified by this prior analysis from the UK Biobank. We found that mean FCHI was negatively correlated with importance rank (Fig. 4C, Spearman r=−0.648, p<0.001), suggesting that the most important DMN subregions in the human had the least functional homology between species. Specifically, medial temporal system components, which were previously identified as having relatively low importance, were found to have high FCHI, while dorsal medial system components, which were identified as being of high importance, had low FCHI. Consistent with prior work suggesting divisions within the core subsystem with respect to high versus low importance, we found that vMPFC and DLPFC exhibited a higher FCHI, while temporal parietal junction (TPJ) and PMC had a lower FCHI (Patel et al., 2019). Together this analysis suggests that regions where the FCHI tends to be relatively lower, correspond to locations which in humans tend to be regions that are most important for reflecting global patterns of functional connectivity within the DMN (Kernbach et al., 2018).

While a number of recent studies have identified a “default-like ” transmodal network in nonhuman populations (e.g., macaque, marmoset, rodents), the extent to which this putative network functions in a manner akin to the human DMN remains an open question (Buckner and Margulies, 2019; Ghahremani et al., 2017; Hutchison and Everling, 2012; Mantini et al., 2011; Mantini and Vanduffel, 2013; Stafford et al., 2014). Here, we examined the similarity of functional organization of DMN subregions across species. This was accomplished by comparing gradient profiles in the common joint-embedding space using cosine similarity. Fig. 5A and B illustrates macaque-human similarities among DMN subregions that exceed our sparsity threshold (i.e., top 10% of pairwise human-macaque similarity over the entire cortex). Four DMN subregions in macaque (i.e., hippocampus [HC], vmPFC, dmPFC and vlPFC) were found to have functional organizations similar to those in humans. For each of the macaque DMN subregions, we identified its functional similarity with each vertex on the human cortex based on the degree of correspondence observed in their functional organization (i.e. gradient profile) (Fig. 5C). The macaque-to-human similarity maps seeded in hippocampus, vmPFC, dmPFC and vlPFC exhibited highly similar spatial patterns as human DMN. In contrast, the FCHI indicated low cross-species similarity in the macaque PMC (PCC), angular gyrus (i.e. PG), and retrosplenial cortex (RSC).

Finally, given recent human studies suggesting the DMN is an apex transmodal network, situated at the furthest end of the macroscale sequence (Margulies et al., 2016), we examined the extent to which the DMN candidate regions in macaque may have evolved along the cortical processing hierarchy. To accomplish this, we used the human principal connectivity gradient as the reference hierarchy and computed the distribution of macaque-to-human similarity for each of macaque DMN seeds. As shown in Fig. 5D, in macaques hippocampus, vmPFC, dmPFC and vlPFC in macaque reached the human hierarchy apex, while the LTC, dPFC and dlPFC. PG, PMC and RSC, which in humans are close to the apex of the functional hierarchy, in macaques occupy lower positions in the unimodal to transmodal hierarchy.

3.8. Cross-species homology maps to cognitive functions

Together, our analysis highlights a pattern of increasing cross species differences in functional organization in regions that are thought to be the most transmodal in humans and which serve highly abstract functions. To quantify aspects of human cognition that are often associated with activity within regions of cross species difference, we compared the spatial distribution of the macaque-to-human FCHI to those provided by a large-scale meta-analysis of task fMRI experiments (Yeo et al., 2015). We first grouped the FCHI into 10-percentile bins and generated probability maps for brain activation under each that reflect the most likely cognitive functions. Probability strength for each cognitive component was normalized and averaged within each bin (see Methods). Fig. 6 shows these data in the form of a heat-map, with the components ordered in rows based on the possibility strengths (Margulies et al., 2016; Wang et al., 2019). The higher FCHI regions were associated with sensorimotor components (e.g., “visual ”, “auditory ”, “hand ”, and “face ”) whereas the lower FCHI regions were involved in high-order cognitive functions (e.g. “interoception ”, “emotion ”, “language ”, “reward ” and “dorsal attention ”). The activation for “working memory ”, “inhibition ” and “internal mentation ” were more likely to overlap with the extremes of the low FCHI regions. These findings establish that regions in which human neural organization is most different from recent common ancestors are related to a combination of executive functions and introspective processes, both of which reflect aspects of cognition that are assumed to be reasonably unique to our species.

3.9. The evolutionary surface area expansion and deformation reveals the network hierarchy

So far our analysis has established that regions of maximal cross species difference across humans and macaques, can be understood along a spectrum, from reasonably high levels of similarity in unimodal regions, to relatively low levels of similarity in regions of the transmodal cortex. This pattern was reflected as a functional shift in meta analytic data towards more abstract functions such as working memory or internal mentation that may be considered to be relatively unique to humans (Margulies et al., 2016). Theories such as the tethering hypothesis attempt to account for how the transmodal cortex gains the ability to support abstract functions, by assuming that this emerges from later development in the evolutionary process (Buckner and Krienen, 2013). To understand whether our index of cross-species similarity captures this hypothesized aspect of evolutionary change, our final analysis examined the correspondence between regions that are assumed to have expanded through evolution with the distribution of the FCHI. We first mapped the relative macaque-to-human changes in cortical area to the cortex (Fig. 7B). Sensory cortices expanded the least whereas the DMN and frontoparietal network expanded more than 20 times from macaque to human (Fig. 7B and C). In particular, the frontal cortex, temporoparietal junction, lateral temporal cortex, and the medial parietal cortex expanded the most from macaque to human. In addition, the spatial map describing surface area expansion is significantly correlated with the FCHI map (r=−.483, p<0.001 corrected) indicating that regions that have expanded the most in human are also those with the least cross species similarity as defined by the FCHI. To demonstrate the evolutionary expansion direction more explicitly, we visualized the macaque- to-human deformation vectors on the human inflated surface (Fig. 7A, center). In this figure the arrows describe the direction of change, and the

color represents the degree of deformation. From macaque to human, the substantial expansion of the frontal cortex appears to push the parietal central regions in a posterior direction. The expansion of TPJ and LTC forced the temporal cortex to move posteriorly and occipital visual cortex is then squeezed into the medial side from macaque to human.

4. Discussion

In this study, we used joint-embedding to create a common space that allowed us to assess the evolutionary changes in functional organization between species. In particular, we demonstrated differences in brain organization that have emerged through evolution can be understood in terms of variation along a hierarchy that reflects the transition of unimodal-transmodal systems. Our results reveal important clues as to how and why human cognition may differ from our close evolutionary ancestors.

We developed a Functional Connectivity Homology Index (FCHI) to quantify the likelihood that anatomically homologous regions share a common functional organization across species. At a global level, the topography of FCHI for humans and macaques had greater similarity in unimodal regions and lower similarity in systems linked to attention and more complex aspects of higher order cognition (Ardesch et al., 2019; Buckner and Krienen, 2013; Burt et al., 2018; Huntenburg et al., 2017). A more fine-grained analysis revealed important distinctions were present within canonical circuits in visual and sensory-motor territories. In these more specialized areas of cortex, we observed that the landmarks tend to fall in regions that were a local maximum for cross-species similarity, and that cross-species similarity declines in adjacent regions following well described local hierarchies (Buckner and Krienen, 2013; Kaas, 2012b; Krubitzer, 2009). This underscores the value of the landmark approach for identifying how systems directly concerned with input and output systems vary across species, while simultaneously highlighting the value of joint embedding as a means to describe functional similarity in other regions of cortex (Mars et al., 2018b; Van Essen and Dierker, 2007). Finally, we also found that the FCHI describes progressively greater differences across species in regions in which neural processing is thought to be important for more complex aspects of human cognition (e.g. attention, memory, internal mentation). Overall, our results establish that important features of the unimodal-transmodal hierarchy that have been observed in humans have emerged through evolution. This raises a number of important issues for our understanding how the organization of the cortex gives rise to uniquely human cognition.

First, using the FCHI as an index of evolutionary conservation, the present study provided clear support for mosaicism in the evolution of the human cortex, which suggests that evolutionary changes are not simultaneous across brain regions (Barton and Harvey, 2000; Gómez-Robles et al., 2014; Smaers and Soligo, 2013). Rather than simply differing across brain “modules ” or networks, the FCHI varied in a systematic fashion both between and within modules, notably in both cases indexing a hierarchical relationship. Locally within unimodal visual and sensorimotor cortical systems, the FCHI decreased away from points of well documented correspondence across species (Buckner and Krienen, 2013; García-Cabezas and Zikopoulos, 2019). Globally the FCHI showed a consistent spatial variation with cortical myelin that increased in the networks anchored in the unimodal cortex and

decreased in networks that are important higher order functions (Margulies et al., 2016; Paquola et al., 2019). Within the DMN those regions with low FCHI are the same regions that in humans contain the most information about global brain dynamics. Together these results are consistent with a complex view of cross-species differentiation which impacts on cortical modules at both a local and global scale. They also highlight that at least parts of the mechanisms that lead to the apparent mosaic-like changes in cortical organization that emerged through evolution is also reflected in the neural hierarchy observed in humans (Burt et al., 2018; Goulas et al., 2014; Paquola et al., 2019; Sneve et al., 2018; Wang et al., 2019).

Second, the distribution of cross-species similarities identified by the FCHI is consistent with the tethering hypothesis (Buckner and Krienen, 2013; Kaas, 2012b; Krubitzer, 2009). We found that both the early visual cortex and the ventral visual pathway anchored from V1, and the hierarchy organization seen in MT and neighboring areas, were reflected as decreases in the FCHI. The tethering hypothesis suggests new functional capabilities have arisen through the gradual duplication, budding, and subdivision of brain areas (Buckner and Krienen, 2013). Specifically, through a process of cortical expansion, large parts of the cortical mantle are postulated to have progressively become untethered from direct roles in input and output system as they become increasingly distant from the constraints of molecular gradients that surrounded key “anchor ” regions (e.g., V1 and MT) (Buckner and Krienen, 2013; Rosa, 2002; Van Essen et al., 2018). We found that the FCHI reflects this hierarchy at both the local and global scale. For example, in canonical circuits in sensory and motor cortex, the observed radial pattern in the FCHI supports the view that evolutionary changes are increasingly important outside of the primary cortex. We also found the FCHI was lower in regions in which cortical expansion across species is thought to be largest (Mars et al., 2018b; Van Essen et al., 2018). Taken together, our findings support the tethering hypothesis in multiple functional aspects.

Third, our study provides important insight into the evolution of the commonly described DMN as is seen in humans. We found that nodes within the DMN show an important differential relationship in terms of their cross-species similarity. In particular, while some DMN regions are functionally similar in both species, two core regions of the DMN exhibited low similarity between humans and macaques: the PMC (PCC-PCU) and PG (parietal gyrus and angular gyrus). In contrast, the vmPFC shows a more similar organizational profile across species (Amiez et al.; Ghahremani et al., 2017). In humans it has recently been established that these regions with the lowest FCHI (e.g. PG and PCC) provide the greatest information about connectome wide patterns of information flow (Kernbach et al., 2018). Moreover, recent task-fMRI studies have determined that these regions can play a crucial role in the application of task-relevant information during working memory and cognitive flexibility tasks (Murphy et al., 2019, 2018; Vatansever et al., 2017). Together these results suggest that in functional terms, some aspects of what is called the default mode in humans are present in macaques, while others, particularly the posterior regions, have a much more unique functional profile in humans (Andrews-Hanna et al., 2014; Kernbach et al., 2018). One implication of the distribution of the FCHI across the DMN is that while the foundations of this system may be present in many species, the pattern seen in humans in which both anterior and posterior regions act in concert, may have emerged relatively later during human evolution. As a consequence, the functional pattern

that represents the DMN as seen in humans, may be present in only a subset of our recent ancestors. It is also possible that these, as well as higher nonhuman primate species (e.g., chimpanzee) would exhibit transitional or intermediate DMN variants.

There are a number of issues that should be considered when interpreting our results. Our cross species joint-embedding is part of an emerging trend toward the use of common high-dimensional spaces as a tool to understand the evolutionary changes across species. Recent efforts have developed strategies for alignment based on white matter tracts, or myelin (T1w/T2w) maps (Eichert et al., 2019; Mars et al., 2018b), as well as task-based activations during movie viewing (Mantini et al., 2012). We anticipate that the joint-embedding approach used in this paper should be readily extensible to diffusion imaging data and encourage future work in this direction (Mars et al., 2018a, 2016). Regardless of which data modality is used, the use of a high-dimensional common space may help characterize functional similarities and differences across species, particularly in areas where clear anatomical landmarks are difficult or impossible to ascertain. In principle, this approach could be extended to multiple species (e.g., chimpanzee, baboon, marmoset etc.) to allow alignment across multiple non-human species including human primates, as well as other mammals, for example rodents. Future work using multimodal imaging in multiple species is required to disentangle function and anatomy in our understanding of brain evolution and development (Heuer et al., 2019; Heuer and Toro, 2019). It is also important to note that our analyses were carried out at the group-level. This decision was motivated by our desire to maximize signal to noise ratio, though proper implementation of this method in individual animals will require the additional optimization of methods (e.g., sufficient data collection for individual dataset, generation of individual-specific landmark masks) (Croxson et al., 2018; Xu et al., 2019, 2018). In addition, while the present work addressed issues regarding the reproducibility of findings by replicating analyses in independent samples, our understanding of their functional significance is based on a meta-analysis and so the precise functional meaning of the observed differences remains largely a matter of conjecture (Braga and Buckner, 2017; Laumann et al., 2015). In order to fully appreciate the significance of these cross-species differences in brain organization for human cognition, it will be necessary to understand how these patterns change across contexts, and, if possible, during active tasks states (Petit and Pouget, 2019; Sharma et al., 2019). Understanding how functional patterns change across a common embedded space during periods of task engagement, could provide invaluable insight into how evolution has shaped many important aspects of human cognition (Murphy et al., 2018).

In summary, our results provide novel insights into the mode in which evolutionary changes sculpt the cerebral cortex layout. Using the FCHI, a quantitative index of neural similarity across species, we established that important changes in how cortical regions communicate has emerged in a progressive fashion along the spectrum spanned by unimodal and transmodal regions, which reflect the structural and functional gradients that pertain to the human cerebral cortex. Importantly, our findings highlight the way that evolutionary changes might have contributed to the emergence of uniquely human higher-order cognition, and provide potential insights into the evolutionary roots of sub- systems within the attention, frontoparietal and default mode networks. Additionally, the posterior DMN, as the apex of a

cognitive hierarchy, may have unique evolutionary adaptations and changed substantially from the most recent common ancestor of humans and macaques.

Supplementary Material

Refer to Web version on PubMed Central for supplementary material.

Acknowledgments

This work was supported by gifts from Joseph P. Healey, Phyllis Green, and Randolph Cowen to the Child Mind Institute and the NIH BRAIN Initiative R01-MH111439 to C.E.S and M.P.M.; R24 MH114806 to M.P.M.; NIH NIBIB NAC P41EB015902, Austrian Science Fund FWF I2714-B31, and the EU H2020 765148 TRABIT to G.L.; NSF EEC-1707298 and Microsoft Research support to J.T.V.; ERC Consolidator award WANDERINGMINDS 646927 to J.S.; CNRS PICS Grant 288256 to D.S.M.; RF1MH117428 to T.X and P50 MH109429 to C.E.S.; and Oesterreichische Nationalbank support (OeNB16725) to K-H.N.; We would also like to thank the investigative teams from Oxford (J. Sallet, R.B. Mars, M.F.S. Rushworth), Newcastle (J. Nacef, C.I. Petkov, F. Balezeau, T.D. Griffiths, C. Poirier, A. Thiele, M. Ortiz, M. Schmid, D. Hunter) and UC-Davis (M. Baxter, P. Croxson, J. Morrison), as well as the funding agencies that make their work possible (Oxford: Wellcome Trust, Royal Society, Medical Research Council, UK Biotechnology Biological Sciences Research Council; Newcaste: National Center for 3Rs, NIH, Wellcome Trust, UK Biotechnology Biological Sciences Research Council; UC-Davis: NIA).

References

Almécija S, Smaers JB, Jungers WL, 2015 The evolution of human and ape hand proportions. Nat. Commun 6, 7717. [PubMed: 26171589]

Amiez C, Sallet J, Hopkins WD, Meguerditchian A, Hadj-Bouziane F, BenHamed S, Wilson CRE, Procyk E, Petrides M, Sulcal organization in the Medial Frontal Cortex Reveals Insights into Primate Brain Evolution. 10.1101/527374.

Andrews-Hanna JR, Reidler JS, Sepulcre J, Poulin R, Buckner RL, 2010 Functional-anatomic fractionation of the brain's default network. Neuron 65, 550–562. [PubMed: 20188659]

Andrews-Hanna JR, Smallwood J, Spreng RN, 2014 The default network and self-generated thought: component processes, dynamic control, and clinical relevance. Ann. N. Y. Acad. Sci 1316, 29–52. [PubMed: 24502540]

Ardesch DJ, Scholtens LH, Li L, Preuss TM, Rilling JK, van den Heuvel MP, 2019 Evolutionary expansion of connectivity between multimodal association areas in the human brain compared with chimpanzees. Proc. Natl. Acad. Sci doi: 10.1073/pnas.1818512116.

Autio JA, Glasser MF, Ose T, Donahue CJ, Bastiani M, 2019 Towards HCP-Style Macaque Connectomes: 24-Channel 3T Multi-Array Coil, MRI Sequences and Preprocessing. bioRxiv

Barton RA, Harvey PH, 2000 Mosaic evolution of brain structure in mammals. Nature 405, 1055–1058. [PubMed: 10890446]

Baumann S, Griffiths TD, Sun L, Petkov CI, Thiele A, Rees A, 2011 Orthogonal representation of sound dimensions in the primate midbrain. Nat. Neurosci 14, 423–425. [PubMed: 21378972]

Baumann S, Joly O, Rees A, Petkov CI, Sun L, Thiele A, Griffiths TD, 2015 The topography of frequency and time representation in primate auditory cortices. Elife 4. doi: 10.7554/elife.03256.

Berwick RC, Friederici AD, Chomsky N, Bolhuis JJ, 2013 Evolution, brain, and the nature of language. Trends Cogn. Sci 17, 89–98. [PubMed: 23313359]

Braga RM, Buckner RL, 2017 Parallel interdigitated distributed networks within the individual estimated by intrinsic functional connectivity. Neuron 95, 457–471 e5. [PubMed: 28728026]

Buckner RL, Krienen FM, 2013 The evolution of distributed association networks in the human brain. Trends Cogn. Sci 17, 648–665. [PubMed: 24210963]

Buckner RL, Margulies DS, 2019 Macroscale cortical organization and a default-like apex transmodal network in the marmoset monkey. Nat. Commun doi: 10.1038/s41467-019-09812-8.

Burt JB, Demirta ş M, Eckner WJ, Navejar NM, Ji JL, Martin WJ, Bernacchia A, Anticevic A, Murray JD, 2018 Hierarchy of transcriptomic specialization across human cortex captured by structural neuroimaging topography. Nat. Neurosci 21, 1251–1259. [PubMed: 30082915]

Byrne RW, 1995 The Thinking Ape: Evolutionary Origins of Intelligence. Oxford University Press.

Caspari N, Janssens T, Mantini D, Vandenberghe R, Vanduffel W, 2015 Covert shifts of spatial attention in the macaque monkey. J. Neurosci doi: 10.1523/jneurosci.4383-14.2015.

Chaplin TA, Yu H-H, Soares JGM, Gattass R, Rosa MGP, 2013 A conserved pattern of differential expansion of cortical areas in simian primates. J. Neurosci 33, 15120–15125. [PubMed: 24048842]

Coifman RR, Lafon S, 2006 Diffusion maps. Applied and Computational Harmonic Analysis 10.1016/j.acha.2006.04.006.

Croxson PL, Forkel SJ, Cerliani L, Thiebaut de Schotten M, 2018 Structural variability across the primate brain: a cross-species comparison. Cereb. Cortex 28, 3829–3841. [PubMed: 29045561]

Dixon ML, De La Vega A, Mills C, Andrews-Hanna J, Spreng RN, Cole MW, Christoff K, 2018 Heterogeneity within the frontoparietal control network and its relationship to the default and dorsal attention networks. Proc. Natl. Acad. Sci. USA 115, E1598–E1607. [PubMed: 29382744]

Donahue CJ, Glasser MF, Preuss TM, Rilling JK, Van Essen DC, 2018 Quantitative assessment of prefrontal cortex in humans relative to nonhuman primates. Proc. Natl. Acad. Sci. USA 115, E5183–E5192. [PubMed: 29739891]

Donahue CJ, Sotiropoulos SN, Jbabdi S, Hernandez-Fernandez M, Behrens TE, Dyrby TB, Coalson T, Kennedy H, Knoblauch K, Van Essen DC, Glasser MF, 2016 Using diffusion tractography to predict cortical connection strength and distance: a quantitative comparison with tracers in the monkey. J. Neurosci 36, 6758–6770. [PubMed: 27335406]

Eichert N, Robinson EC, Bryant KL, Jbabdi S, 2019 Cross-species Cortical Alignment Identifies Different Types of Neuroanatomical Reorganization in Higher Primates. bioRxiv.

Felleman DJ, Van Essen DC, 1991 Distributed hierarchical processing in the primate cerebral cortex. Cereb. Cortex doi: 10.1093/cercor/1.1.1.

Ferry AT, Ongür D, An X, Price JL, 2000 Prefrontal cortical projections to the striatum in macaque monkeys: evidence for an organization related to prefrontal networks. J. Comp. Neurol 425, 447–470. [PubMed: 10972944]

García-Cabezas MÁ, Zikopoulos B, 2019 Evolution, development, and organization of the cortical connectome. PLoS Biol 17, e3000259. [PubMed: 31075099]

Ghahremani M, Hutchison RM, Menon RS, Everling S, 2017 Frontoparietal functional connectivity in the common marmoset. Cereb. Cortex 27, 3890–3905. [PubMed: 27405331]

Glasser MF, Coalson TS, Robinson EC, Hacker CD, Harwell J, Yacoub E, Ugurbil K, Andersson J, Beckmann CF, Jenkinson M, Smith SM, Van Essen DC, 2016 A multi-modal parcellation of human cerebral cortex. Nature 536, 171–178. [PubMed: 27437579]

Glasser MF, Sotiropoulos SN, Wilson JA, Coalson TS, Fischl B, Andersson JL, Xu J, Jbabdi S, Webster M, Polimeni JR, Van Essen DC, Jenkinson M WU-Minn HCP Consortium, 2013 The minimal preprocessing pipelines for the human connectome project. Neuroimage 80, 105–124. [PubMed: 23668970]

Glasser MF, Van Essen DC, 2011 Mapping human cortical areas in vivo based on myelin content as revealed by T1- and T2-weighted MRI. J. Neurosci 31, 11597–11616. [PubMed: 21832190]

Gómez-Robles A, Hopkins WD, Sherwood CC, 2014 Modular structure facilitates mosaic evolution of the brain in chimpanzees and humans. Nat. Commun 5, 4469. [PubMed: 25047085]

Goulas A, Bastiani M, Bezgin G, Uylings HBM, Roebroeck A, Stiers P, 2014 Comparative analysis of the macroscale structural connectivity in the macaque and human brain. PLoS Comput. Biol 10, e1003529. [PubMed: 24676052]

Haak KV, Marquand AF, Beckmann CF, 2018 Connectopic mapping with resting-state fMRI. Neuroimage 170, 83–94. [PubMed: 28666880]

Hage SR, Nieder A, 2016 Dual neural network model for the evolution of speech and language. Trends Neurosci 39, 813–829. [PubMed: 27884462]

Heuer K, Gulban OF, Bazin P-L, Osoianu A, Valabregue R, Santin M, Herbin M, Toro R, 2019 Evolution of neocortical folding: A phylogenetic comparative analysis of MRI from 34 primate species. Cortex. doi: 10.1016/j.cortex.2019.04.011.

Heuer K, Toro R, 2019 Role of mechanical morphogenesis in the development and evolution of the neocortex. Phys. Life Rev 31, 233–239. [PubMed: 30738760]

Hill J, Inder T, Neil J, Dierker D, Harwell J, Van Essen D, 2010 Similar patterns of cortical expansion during human development and evolution. Proc. Natl. Acad. Sci. USA 107, 13135–13140. [PubMed: 20624964]

Hopkins WD, Meguerditchian A, Coulon O, Bogart S, Mangin J-F, Sherwood CC, Grabowski MW, Bennett AJ, Pierre PJ, Fears S, Woods R, Hof PR, Vauclair J, 2014 Evolution of the central sulcus morphology in primates. Brain Behav. Evol 84, 19–30. [PubMed: 25139259]

Huntenburg JM, Bazin P-L, Goulas A, Tardif CL, Villringer A, Margulies DS, 2017 A systematic relationship between functional connectivity and intracortical myelin in the human cerebral cortex. Cereb. Cortex 27, 981–997. [PubMed: 28184415]

Hutchison RM, Everling S, 2012 Monkey in the middle: why non-human primates are needed to bridge the gap in resting-state investigations. Front. Neuroanat 6, 29. [PubMed: 22855672]

Kaas JH, 2012a The evolution of neocortex in primates. Evol. Primate Brain. doi: 10.1016/b978-0-444-53860-4.00005-2.

Kaas JH, 2012b The evolution of neocortex in primates. Prog. Brain Res 195, 91–102. [PubMed: 22230624]

Kernbach JM, Yeo BTT, Smallwood J, Margulies DS, Thiebaut de Schotten M, Walter H, Sabuncu MR, Holmes AJ, Gramfort A, Varoquaux G, Thirion B, Bzdok D, 2018 Subspecialization within default mode nodes characterized in 10,000 UK Biobank participants. Proc. Natl. Acad. Sci. USA 115, 12295–12300. [PubMed: 30420501]

Krubitzer L, 2007 The magnificent compromise: cortical field evolution in mammals. Neuron 56, 201–208. [PubMed: 17964240]

Krubitzer L, 2009 In search of a unifying theory of complex brain evolution. Ann. N. Y. Acad. Sci 1156, 44–67. [PubMed: 19338502]

Langs G, Golland P, Tie Y, Rigolo L, Golby AJ, 2010 Functional geometry alignment and localization of brain areas. Adv. Neural Inf. Process. Syst 1, 1225–1233. [PubMed: 24808719]

Laumann TO, Gordon EM, Adeyemo B, Snyder AZ, Joo SJ, Chen M-Y, Gilmore AW, McDermott KB, Nelson SM, Dosenbach NUF, Schlaggar BL, Mumford JA, Poldrack RA, Petersen SE, 2015 Functional system and areal organization of a highly sampled individual human brain. Neuron 87, 657–670. [PubMed: 26212711]

Lewis JW, Van Essen DC, 2000 Corticocortical connections of visual, sensorimotor, and multimodal processing areas in the parietal lobe of the macaque monkey. J. Comp. Neurol 428, 112–137. [PubMed: 11058227]

Mansouri FA, Koechlin E, Rosa MGP, Buckley MJ, 2017 Managing competing goals —a key role for the frontopolar cortex. Nat. Rev. Neurosci 18, 645. [PubMed: 28951610]

Mantini D, Corbetta M, Romani GL, Orban GA, Vanduffel W, 2013 Evolutionarily novel functional networks in the human brain? J. Neurosci. doi: 10.1523/jneurosci.4392-12.2013.

Mantini D, Gerits A, Nelissen K, Durand J-B, Joly O, Simone L, Sawamura H, Wardak C, Orban GA, Buckner RL, Vanduffel W, 2011 Default mode of brain function in monkeys. J. Neurosci 31, 12954–12962. [PubMed: 21900574]

Mantini D, Hasson U, Betti V, Perrucci MG, Romani GL, Corbetta M, Orban GA, Vanduffel W, 2012 Interspecies activity correlations reveal functional correspondence between monkey and human brain areas. Nat. Methods 9, 277–282. [PubMed: 22306809]

Mantini D, Vanduffel W, 2013 Emerging roles of the brain's default network. Neuroscientist 19, 76–87. [PubMed: 22785104]

Margulies DS, Ghosh SS, Goulas A, Falkiewicz M, Huntenburg JM, Langs G, Bezgin G, Eickhoff SB, Castellanos FX, Petrides M, Jefferies E, Smallwood J, 2016 Situating the default-mode network along a principal gradient of macroscale cortical organization. Proc. Natl. Acad. Sci. USA 113, 12574–12579. [PubMed: 27791099]

Markov NT, Ercsey-Ravasz MM, Ribeiro Gomes AR, Lamy C, Magrou L, Vezoli J, Misery P, Falchier A, Quilodran R, Gariel MA, Sallet J, Gamanut R, Huissoud C, Clavagnier S, Giroud P, Sappey-Marinier D, Barone P, Dehay C, Toroczkai Z, Knoblauch K, Van Essen DC, Kennedy H, 2014 A weighted and directed interareal connectivity matrix for macaque cerebral cortex. Cereb. Cortex 24, 17–36. [PubMed: 23010748]

Mars RB, Foxley S, Verhagen L, Jbabdi S, Sallet J, Noonan MP, Neubert F-X, Andersson JL, Croxson PL, Dunbar RIM, Khrapitchev AA, Sibson NR, Miller KL, Rushworth MFS, 2016 The extreme capsule fiber complex in humans and macaque monkeys: a comparative diffusion MRI tractography study. Brain Struct. Funct 221, 4059–4071. [PubMed: 26627483]

Mars RB, Jbabdi S, Sallet J, O'Reilly JX, Croxson PL, Olivier E, Noonan MP, Bergmann C, Mitchell AS, Baxter MG Others, 2011 Diffusion-weighted imaging tractography-based parcellation of the human parietal cortex and comparison with human and macaque resting-state functional connectivity. J. Neurosci 31, 4087–4100. [PubMed: 21411650]

Mars RB, Neubert F-X, Verhagen L, Sallet J, Miller KL, Dunbar RIM, Barton RA, 2014 Primate comparative neuroscience using magnetic resonance imaging: promises and challenges. Front. Neurosci 8, 298. [PubMed: 25339857]

Mars RB, Passingham RE, Jbabdi S, 2018a Connectivity fingerprints: from areal descriptions to abstract spaces. Trends Cogn. Sci 22, 1026–1037. [PubMed: 30241910]

Mars RB, Sotiropoulos SN, Passingham RE, Sallet J, Verhagen L, Khrapitchev AA, Sibson N, Jbabdi S, 2018b Whole brain comparative anatomy using connectivity blueprints. Elife 7. doi: 10.7554/eLife.35237.

Mesulam M, 1998 From sensation to cognition. Brain. doi: 10.1093/brain/121.6.1013.

Milham MP, Ai L, Koo B, Xu T, Amiez C, Balezeau F, Baxter MG, Blezer ELA, Brochier T, Chen A, Croxson PL, Damatac CG, Dehaene S, Everling S, Fair DA, Fleysher L, Freiwald W, Froudist-Walsh S, Griffiths TD, Guedj C, Hadj-Bouziane F, Ben Hamed S, Harel N, Hiba B, Jarraya B, Jung B, Kastner S, Klink PC, Kwok SC, Laland KN, Leopold DA, Lindenfors P, Mars RB, Menon RS, Messinger A, Meunier M, Mok K, Morrison JH, Nacef J, Nagy J, Rios MO, Petkov CI, Pinsk M, Poirier C, Procyk E, Rajimehr R, Reader SM, Roelfsema PR, Rudko DA, Rushworth MFS, Russ BE, Sallet J, Schmid MC, Schwiedrzik CM, Seidlitz J, Sein J, Shmuel A, Sullivan EL, Ungerleider L, Thiele A, Todorov OS, Tsao D, Wang Z, Wilson CRE, Yacoub E, Ye FQ, Zarco W, Zhou Y-D, Margulies DS, Schroeder CE, 2018 An open resource for non-human primate imaging. Neuron 100, 61–74 e2. [PubMed: 30269990]

Murphy C, Jefferies E, Rueschemeyer S-A, Sormaz M, Wang H-T, Margulies DS, Smallwood J, 2018 Distant from input: evidence of regions within the default mode network supporting perceptually-decoupled and conceptually-guided cognition. Neuroimage 171, 393–401. [PubMed: 29339310]

Murphy C, Wang H-T, Konu D, Lowndes R, Margulies DS, Jefferies E, Smallwood J, 2019 Modes of operation: a topographic neural gradient supporting stimulus dependent and independent cognition. Neuroimage 186, 487–496. [PubMed: 30447291]

Nenning K-H, Liu H, Ghosh SS, Sabuncu MR, Schwartz E, Langs G, 2017 Diffeomorphic functional brain surface alignment: functional demons. Neuroimage 156, 456–465. [PubMed: 28416451]

Neubert F-X, Mars RB, Thomas AG, Sallet J, Rushworth MFS, 2014 Comparison of human ventral frontal cortex areas for cognitive control and language with areas in monkey frontal cortex. Neuron 81, 700–713. [PubMed: 24485097]

Noonan MP, Sallet J, Mars RB, Neubert FX, O'Reilly JX, Andersson JL, Mitchell AS, Bell AH, Miller KL, Rushworth MFS, 2014 A neural circuit covarying with social hierarchy in macaques. PLoS Biol 12, e1001940. [PubMed: 25180883]

Oya T, Takei T, Seki K, 2020 Distinct sensorimotor feedback loops for dynamic and static control of primate precision grip. Commun. Biol 3, 156. [PubMed: 32242085]

Paquola C, Vos De Wael R, Wagstyl K, Bethlehem RAI, Hong S-J, Seidlitz J, Bullmore ET, Evans AC, Misic B, Margulies DS, Smallwood J, Bernhardt BC, 2019 Microstructural and functional gradients are increasingly dissociated in transmodal cortices. PLoS Biol 17, e3000284. [PubMed: 31107870]

Patel GH, Sestieri C, Corbetta M, 2019 The evolution of the temporoparietal junction and posterior superior temporal sulcus. Cortex. doi: 10.1016/j.cortex.2019.01.026.

Patel GH, Yang D, Jamerson EC, Snyder LH, Corbetta M, Ferrera VP, 2015 Functional evolution of new and expanded attention networks in humans. Proc. Natl. Acad. Sci. USA 112, 9454–9459. [PubMed: 26170314]

Paxinos G, Franklin KBJ, 2012 Paxinos and Franklin's the Mouse Brain in Stereotaxic Coordinates. Academic Press.

Petit L, Pouget P, 2019 The comparative anatomy of frontal eye fields in primates. Cortex. doi: 10.1016/j.cortex.2019.02.023.

Poerio GL, Sormaz M, Wang H-T, Margulies D, Jefferies E, Smallwood J, 2017 The role of the default mode network in component processes underlying the wandering mind. Soc. Cogn. Affect. Neurosci 12, 1047–1062. [PubMed: 28402561]

Poirier C, Baumann S, Dheerendra P, Joly O, Hunter D, Balezeau F, Sun L, Rees A, Petkov CI, Thiele A, Griffiths TD, 2017 Auditory motion-specific mechanisms in the primate brain. PLoS Biol 15, e2001379. [PubMed: 28472038]

Preuss TM, Goldman-Rakic PS, 1991 Architectonics of the parietal and temporal association cortex in the strepsirhine primate Galago compared to the anthropoid primate Macaca. J. Comp. Neurol 310, 475–506. [PubMed: 1939733]

Reid AT, Lewis J, Bezgin G, Khundrakpam B, Eickhoff SB, McIntosh AR, Bellec P, Evans AC, 2016 A cross-modal, cross-species comparison of connectivity measures in the primate brain. NeuroImage. doi: 10.1016/j.neuroimage.2015.10.057.

Rilling JK, 2014 Comparative primate neuroimaging: insights into human brain evolution. Trends Cogn. Sci. 18, 46–55. [PubMed: 24501779]

Rinne T, Muers RS, Salo E, Slater H, Petkov CI, 2017 Functional imaging of audio–visual selective attention in monkeys and humans: how do lapses in monkey performance affect cross-species correspondences? Cereb. Cortex 27, 3471–3484. [PubMed: 28419201]

Robinson EC, Jbabdi S, Glasser MF, Andersson J, Burgess GC, Harms MP, Smith SM, Van Essen DC, Jenkinson M, 2014 MSM: a new flexible framework for multimodal surface matching. Neuroimage 100, 414–426. [PubMed: 24939340]

Rosa MGP, 2002 Visual maps in the adult primate cerebral cortex: some implications for brain development and evolution. Braz. J. Med. Biol. Res doi: 10.1590/s0100-879×2002001200008.

Sallet J, Mars RB, Noonan MP, Neubert F-X, Jbabdi S, O'Reilly JX, Filippini N, Thomas AG, Rushworth MF, 2013 The organization of dorsal frontal cortex in humans and macaques. J. Neurosci 33, 12255–12274. [PubMed: 23884933]

Schönwiesner M, Dechent P, Voit D, Petkov CI, Krumbholz K, 2015 Parcellation of human and monkey core auditory cortex with fMRI pattern classification and objective detection of tonotopic gradient reversals. Cereb. Cortex 25, 3278–3289. [PubMed: 24904067]

Sharma S, Mantini D, Vanduffel W, Nelissen K, 2019 Functional specialization of macaque premotor F5 subfields with respect to hand and mouth movements: a comparison of task and resting-state fMRI. NeuroImage. doi: 10.1016/j.neuroimage.2019.02.045.

Slater H, Milne AE, Wilson B, Muers RS, Balezeau F, Hunter D, Thiele A, Griffiths TD, Petkov CI, 2016 Individually customisable non-invasive head immobilisation system for non-human primates with an option for voluntary engagement. J. Neurosci. Methods 269, 46–60. [PubMed: 27189889]

Smaers JB, Soligo C, 2013 Brain reorganization, not relative brain size, primarily characterizes anthropoid brain evolution. Proc. Biol. Sci 280, 20130269. [PubMed: 23536600]

Smallwood J, Tipper C, Brown K, Baird B, Engen H, Michaels JR, Grafton S, Schooler JW, 2013 Escaping the here and now: evidence for a role of the default mode network in perceptually decoupled thought. NeuroImage. doi: 10.1016/j.neuroimage.2012.12.012.

Sneve MH, Grydeland H, Rosa MGP, Paus T, Chaplin T, Walhovd K, Fjell AM, 2018 High-expanding regions in primate cortical brain evolution support supramodal cognitive flexibility. Cereb. Cortex. doi: 10.1093/cercor/bhy268.

Sormaz M, Murphy C, Wang H-T, Hymers M, Karapanagiotidis T, Poerio G, Margulies DS, Jefferies E, Smallwood J, 2018 Default mode network can support the level of detail in experience during active task states. Proc. Natl. Acad. Sci. USA 115, 9318–9323. [PubMed: 30150393]

Sousa AMM, Meyer KA, Santpere G, Gulden FO, Sestan N, 2017 Evolution of the human nervous system function, structure, and development. Cell 170, 226–247. [PubMed: 28708995]

Stafford JM, Jarrett BR, Miranda-Dominguez O, Mills BD, Cain N, Mihalas S, Lahvis GP, Lattal KM, Mitchell SH, David SV, Fryer JD, Nigg JT, Fair DA, 2014 Large-scale topology and the default mode network in the mouse connectome. Proc. Natl. Acad. Sci. USA 111, 18745–18750. [PubMed: 25512496]

Toda T, Kudo T-A, 2015 The ventral primary somatosensory cortex of the primate brain: innate neural interface for dexterous orofacial motor control In: Interface Oral Health Science 2014. Springer, Tokyo, pp. 281–291.

Tsao DY, Moeller S, Freiwald WA, 2008 Comparing face patch systems in macaques and humans. Proc. Natl. Acad. Sci. USA 105, 19514–19519. [PubMed: 19033466]

Ungerleider LG, Haxby JV, 1994 “What ”and “where ”in the human brain. Curr. Opin. Neurobiol 4, 157–165. [PubMed: 8038571]

Van Essen DC, Dierker DL, 2007 Surface-based and probabilistic atlases of primate cerebral cortex. Neuron 56, 209–225. [PubMed: 17964241]

Van Essen DC, Donahue CJ, Glasser MF, 2018 Development and evolution of cerebral and cerebellar cortex. Brain Behav. Evol 91, 158–169. [PubMed: 30099464]

Van Essen DC, Glasser MF, Dierker DL, Harwell J, 2012 Cortical parcellations of the macaque monkey analyzed on surface-based atlases. Cereb. Cortex 22, 2227–2240. [PubMed: 22052704]

Vatansever D, Menon DK, Stamatakis EA, 2017 Default mode contributions to automated information processing. Proc. Natl. Acad. Sci. USA 114, 12821–12826. [PubMed: 29078345]

Wang P, Kong R, Kong X, Liégeois R, Orban C, Deco G, van den Heuvel MP, Thomas Yeo BT, 2019 Inversion of a large-scale circuit model reveals a cortical hierarchy in the dynamic resting human brain. Sci. Adv 5, eaat7854. [PubMed: 30662942]

Wilson B, Kikuchi Y, Sun L, Hunter D, Dick F, Smith K, Thiele A, Griffiths TD, Marslen-Wilson WD, Petkov CI, 2015 Auditory sequence processing reveals evolutionarily conserved regions of frontal cortex in macaques and humans. Nat. Commun 6, 8901. [PubMed: 26573340]

Winkler AM, Sabuncu MR, Yeo BTT, Fischl B, Greve DN, Kochunov P, Nichols TE, Blangero J, Glahn DC, 2012 Measuring and comparing brain cortical surface area and other areal quantities. Neuroimage 61, 1428–1443. [PubMed: 22446492]

Xu T, Falchier A, Sullivan EL, Linn G, Ramirez JSB, Ross D, Feczko E, Opitz A, Bagley J, Sturgeon D, Earl E, Miranda-Domínguez O, Perrone A, Craddock RC, Schroeder CE, Colcombe S, Fair DA, Milham MP, 2018 Delineating the macroscale areal organization of the macaque cortex in vivo. Cell Rep 23, 429–441. [PubMed: 29642002]

Xu T, Sturgeon D, Ramirez JSB, Froudist-Walsh S, Margulies DS, Schroeder CE, Fair DA, Milham MP, 2019 Inter-individual variability of functional connectivity in awake and anesthetized rhesus monkeys. Biol. Psychiatry: Cogn. Neurosci. Neuroimaging 4 (6), 543–553.

Xu T, Yang Z, Jiang L, Xing X-X, Zuo X-N, 2015 A connectome computation system for discovery science of brain. Sci Bull. Fac. Agric. Kyushu Univ 60, 86–95.

Yeo BTT, Krienen FM, Eickhoff SB, Yaakub SN, Fox PT, Buckner RL, Asplund CL, Chee MWL, 2015 Functional specialization and flexibility in human association cortex. Cereb. Cortex 25, 3654–3672. [PubMed: 25249407]

Yeo BTT, Krienen FM, Sepulcre J, Sabuncu MR, Lashkari D, Hollinshead M, Roffman JL, Smoller JW, Zöllei L, Polimeni JR, Fischl B, Liu H, Buckner RL, 2011 The organization of the human cerebral cortex estimated by intrinsic functional connectivity. J. Neurophysiol 106, 1125–1165. [PubMed: 21653723]

Yovel G, Freiwald WA, 2013 Face recognition systems in monkey and human: are they the same thing? F1000Prime Rep 5, 5–10. [PubMed: 23513177]

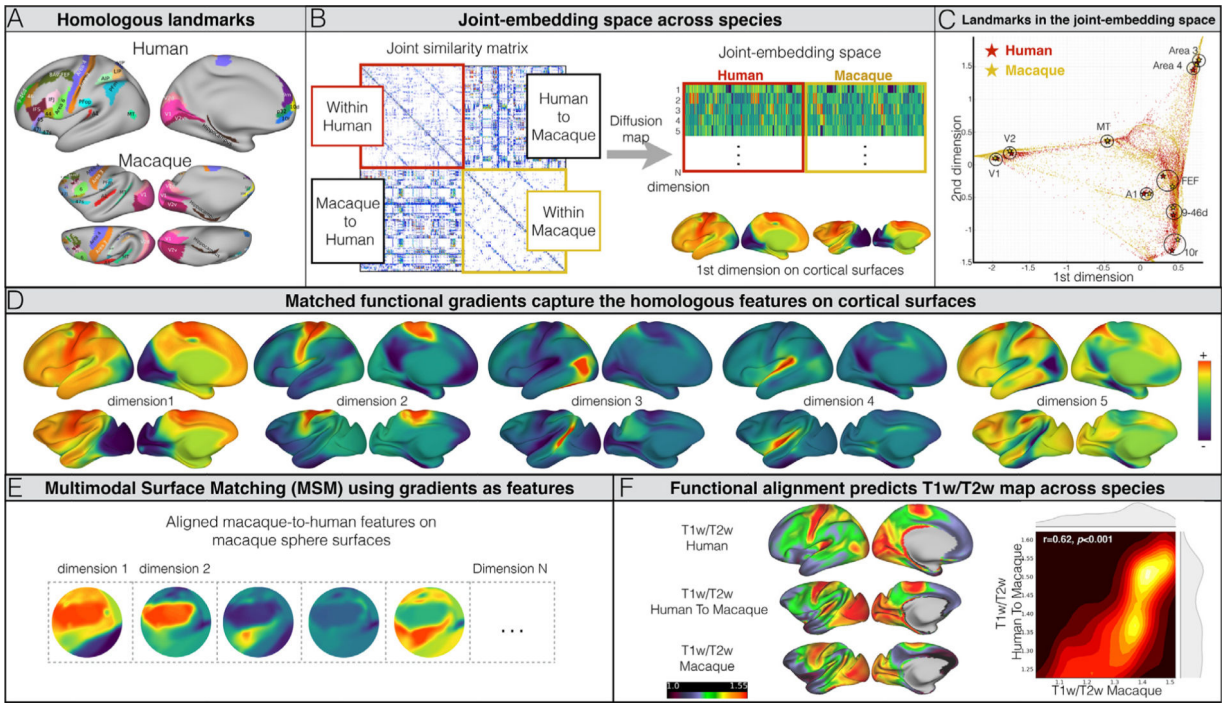

Fig. 1.

Joint-embedding captures the common brain architecture between human and macaque monkey. A) Cross-species homologous landmarks defined by previous studies (Supplementary Table S1). B) Schematic diagram for constructing the cross-species functional common space. The joint-similarity matrix is concatenated by the vertex-wise within-species similarity matrix (diagonal) and between-species similarity matrix (off-diagonal). Spectral embedding was applied on the joint similarity matrix to extract N number of the matched components to construct the cross-species common space. C) Homologous landmark pairs are close in the joint-embedding space (Supplementary Fig. S2). D) Matched components (i.e. gradients on cortex) on human and macaque cortical surfaces highlight the homologous areas. E) The gradients were used as features in MSM for cortical surface alignment on sphere surfaces. F) The established alignment can predict the T1w/T2w map based on the other species. As visualized in a 2D density plot, the T1w/T2w in macaque (x-axis) shows significant spatial correlation with the human-to-macaque T1w/T2w prediction (y-axis).

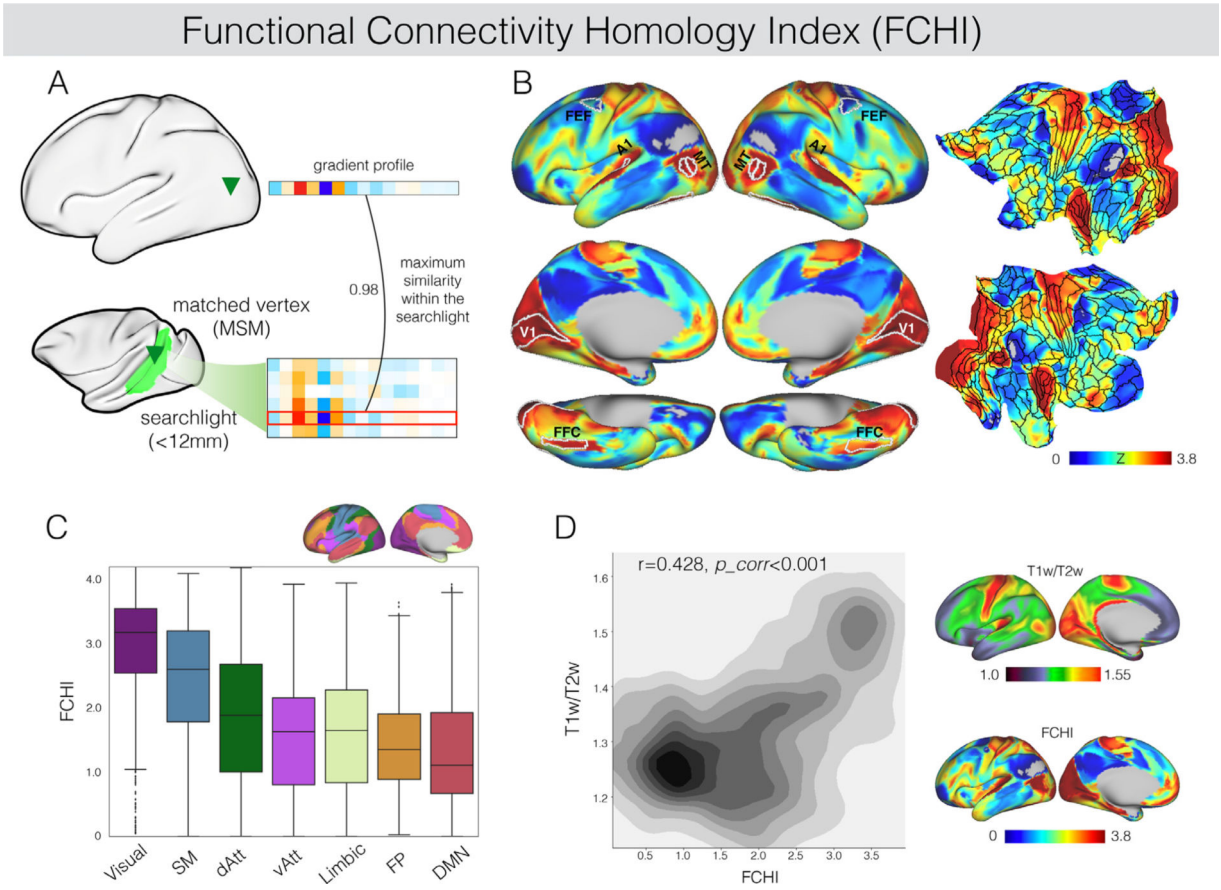

Fig. 2.

The functional homology index (FCHI) reveals the cross-species similarity in network hierarchy. A) FCHI is calculated as the local maximum similarity of the functional gradients profile across species within corresponding searchlights (geodesic distance < 12 mm from the MSM matched vertex). B) FCHI exhibits high values in sensory cortices (e.g. visual, auditory, somatomotor), and lower in high-order association regions. C) FCHI reveals the network hierarchy (Yeo2011 networks). D) The spatial pattern of FCHI is significantly associated with the T1w/T2w map in human.

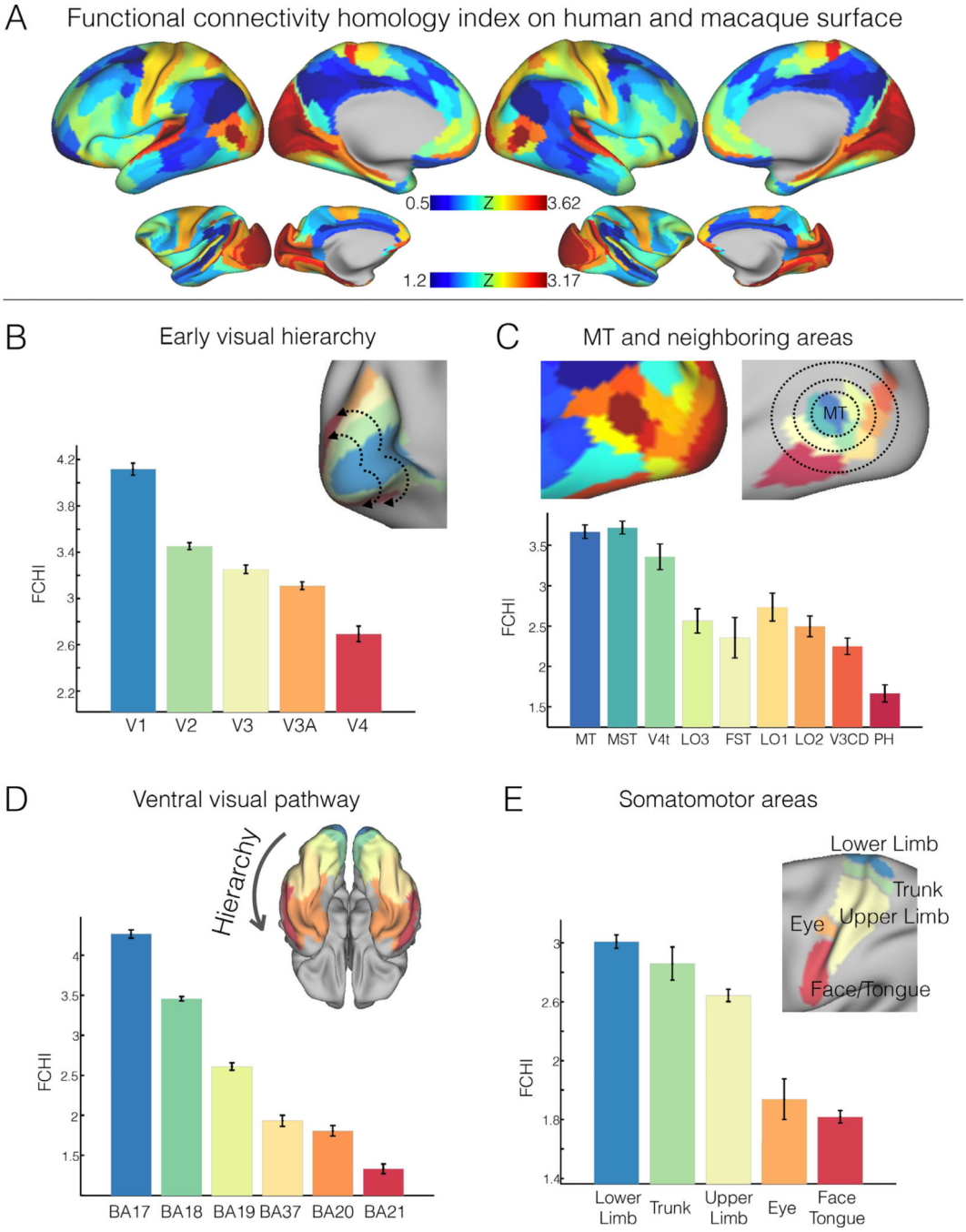

Fig. 3.

Cross-species functional homology index characterizes distributed local sensory hierarchies. A) Parcel-wise FCHI maps in human and macaque monkey based on the recent parcellations (human: Glasser et al., 2016; macaque: Markov et al., 2014). B) FCHI reflects the hierarchy in the early visual processing system. Five areas defined by the Glasser parcellation are rendered on the surface and comprise the early visual areas ordered by the hierarchical streams of eccentricity mapping on x-axis (V1, V2, V3, V3A, V4). C) FCHI exhibits the highest scores in MT and MST with lower scores in MT neighboring areas (x-axis: ordered

by the geodesic distance from MT area). D) FCHI decreases along the ventral visual processing hierarchy (BA17, BA18, BA19, BA37, BA20, BA 21). E) FCHI map varies along the dorsal-ventral axis of somatotopic mapping. The FCHI was averaged within labeled areas and visualized with 95% confidence intervals.

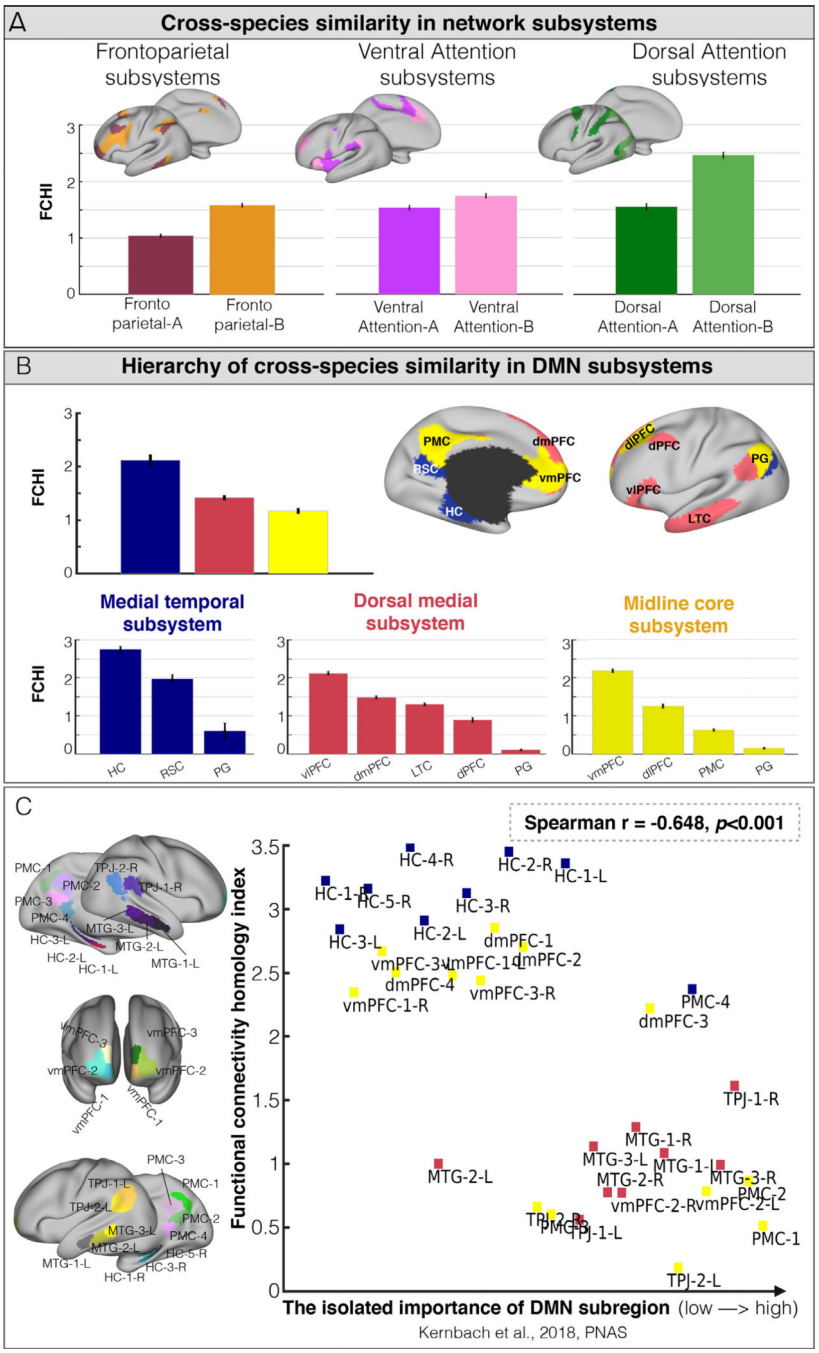

Fig. 4.

The functional homology index reveals the hierarchy of subsystems in the attention, frontoparietal and default mode networks. A) The FCHI shows lower scores in subsystem-A and higher scores in subsystem-B for dorsal attention, ventral attention and frontoparietal networks. B) FCHI differs among subsystems of the default mode network; the core DMN shows the lowest score, dorsal medial system an intermediate score, and medial temporal the highest score. Within each of the subsystems, the PG, PMC and LTC have the lowest FCHI scores. C) FCHI is associated with the level of 'importance' across subregions within the

DMN (Spearman r=−0.648, p<0.001). The importance of the DMN subregions is established by a recent study based on the UK Biobank data.

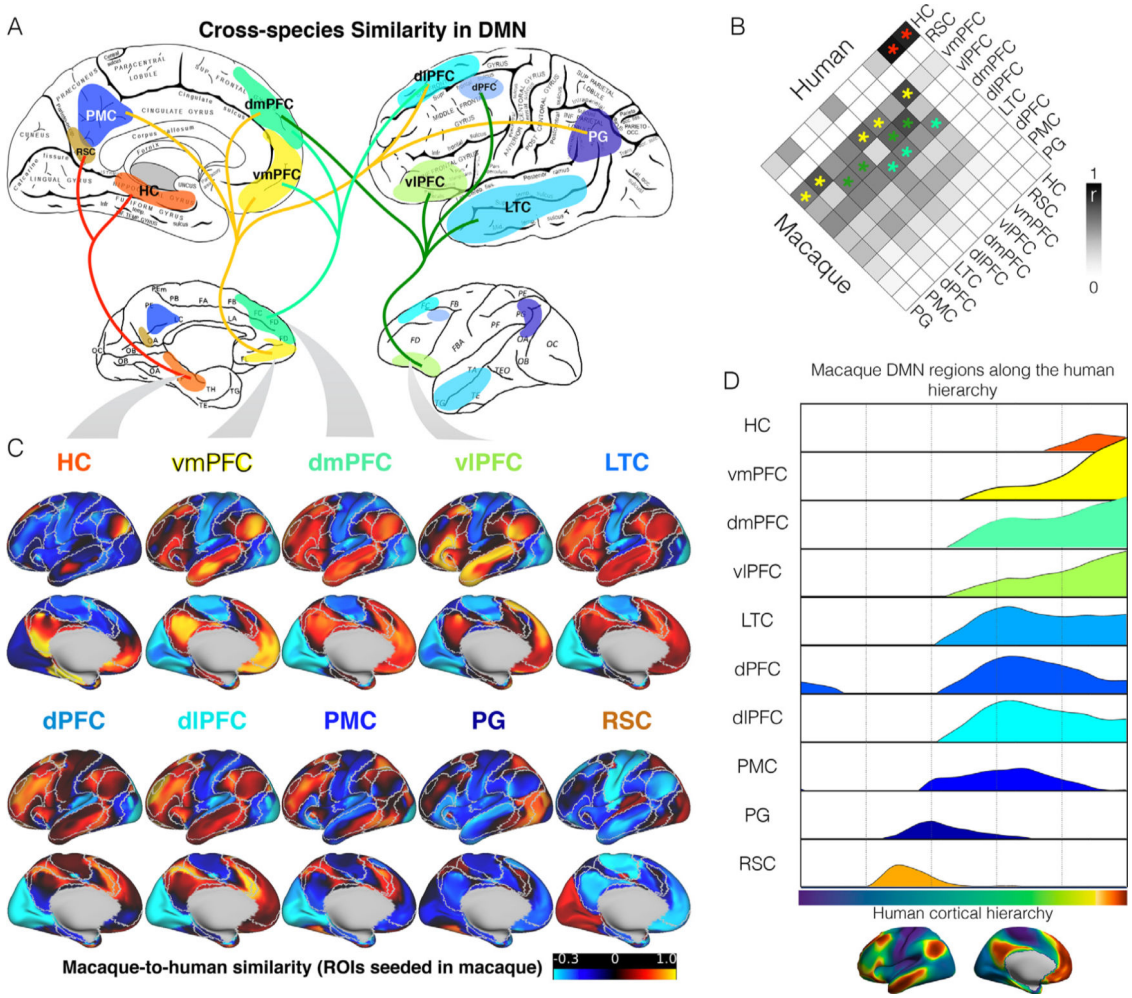

Fig. 5.

The cross-species similarity between humans and macaque monkeys. A) The human-macaque similarity of functional gradient profiles among DMN candidate subregions. The links in the diagram illustrate the similarity among DMN subregions that exceed the sparsity threshold (top 10% of pairwise human-macaque similarity across the entire cortex). B) The pairwise similarity matrix (cosine similarity) of DMN candidate subregions between humans and macaques. C) The cross-species similarity maps (cosine similarity) for each DMN candidate region seeded in macaque. The macaque-to-human similarity maps of HC, vmPFC, dmPFC and dlPFC regions show highly similar spatial patterns as human DMN (white border based on Yeo2011 networks). D) The macaque-to-human similarity maps are represented along the human principle connectivity gradient obtained based on the human HCP sample. Each line of the macaque DMN seed is smoothed by the locally weighted scatterplot smoothing (LOWESS) kernel. The positive distribution is visualized to explicitly demonstrate the extent to which DMN candidate regions in the macaque reached the human hierarchy apex.

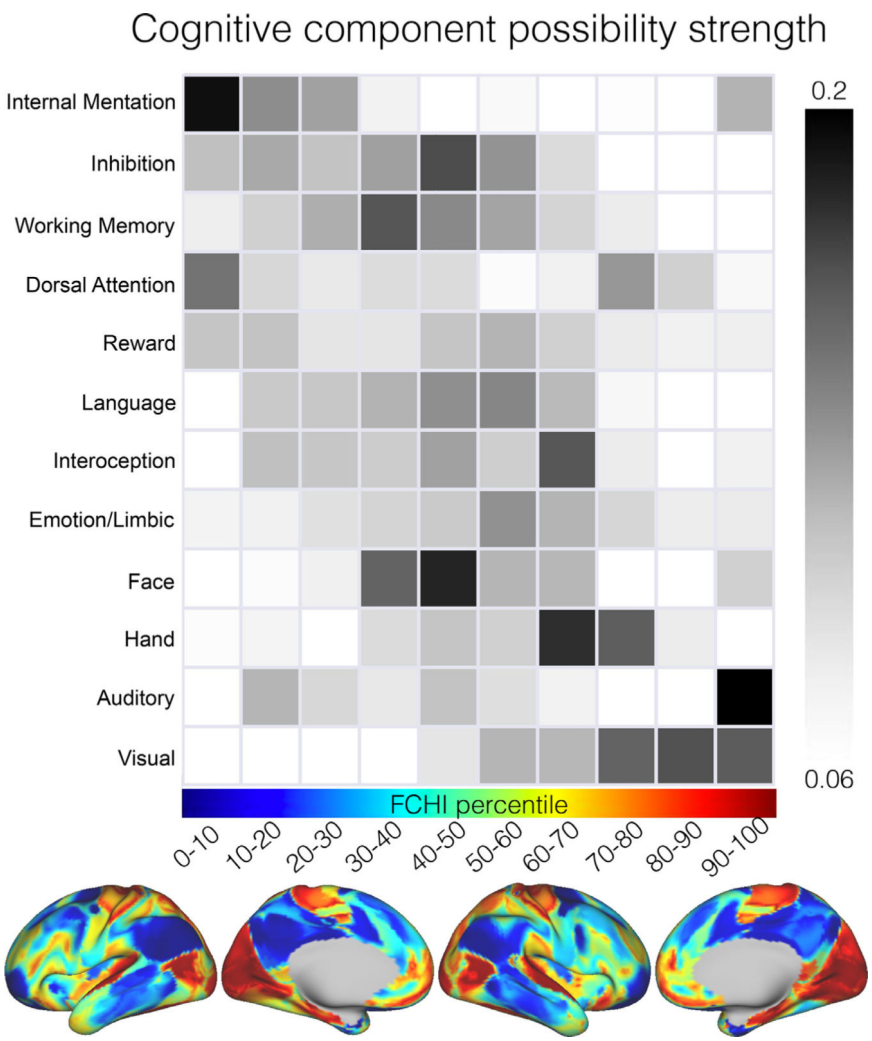

Fig. 6.

Cross-species functional connectivity homology maps to the cognitive functions. Relationship between the FCHI map and twelve cognitive components based on the BrainMap meta-analysis database (Materials and Methods). In rows, the percentiles of the FCHI map are ordered from low to high. In columns, the cognitive components are ordered based on the normalized activation possibility strength weighted by the log scale of percentile. The higher FCHI regions were associated with sensorimotor components whereas the lower FCHI regions were involved in high-order cognitive functions.

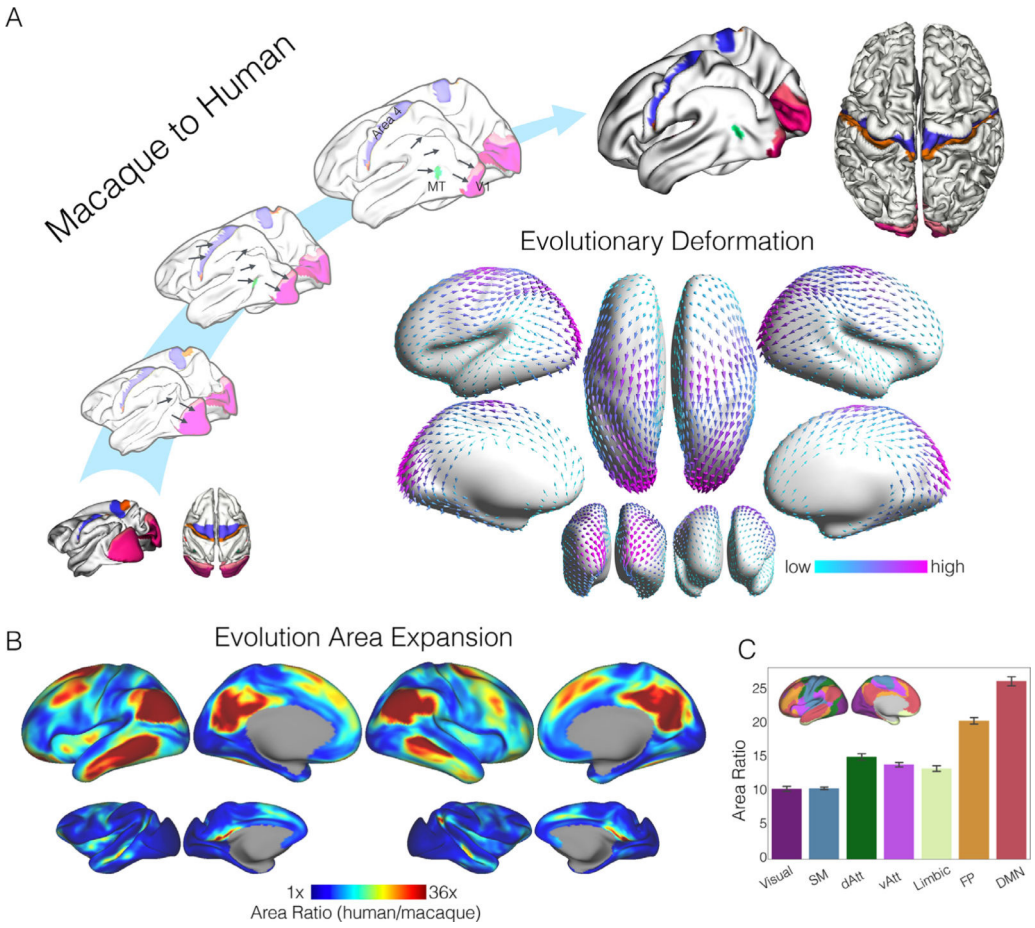

Fig. 7.

Evolutionary surface area expansion and deformation reveals the network hierarchy. A) Schematic diagram illustrating the evolutionary expansion from the macaque monkey to the human. Homologous anchors in somatomotor (area 3, area 4), primary visual areas (V1, V2) and MT areas were labeled on individual macaque and human surfaces, as well as the intermediate surfaces from macaque to human. Evolutionary expansion direction (i.e. macaque-to-human deformation vectors) is visualized in arrows on the human inflated surface (center). B) Surface areal expansion maps were calculated as the human area divided by macaque area at each of corresponding vertex on human and macaque surfaces. C) Sensory cortices expanded the least (10 times), whereas the high-order association cortex expanded the most from the macaque to the human.